universität wien

MASTERARBEIT / MASTER'S THESIS

Titel der Masterarbeit / Title of the Master's Thesis

„Employing 5-hydroxy-[1,4]-naphthoquinones as bioactive ligand scaffolds for organometallic complexes“

verfasst von / submitted by

Manuel Pristner, BSc

angestrebter akademischer Grad / in partial fulfilment of the requirements for the degree of

Master of Science (MSc)

Wien, 2018 / Vienna 2018

Studienkennzahl lt. Studienblatt / degree programme code as it appears on the student record sheet:	A 066 862
Studienrichtung lt. Studienblatt / degree programme as it appears on the student record sheet:	Masterstudium Chemie
Betreut von / Supervisor:	O. Univ.-Prof. Dr. Dr. Bernhard K. Keppler
Mitbetreut von / Co-Supervisor:	Dipl.-Ing. Dr. Wolfgang Kandioller

Acknowledgment

I want to thank all the people who helped me during my master thesis:

O. Univ.-Prof. Dr. Dr. Bernhard K. Keppler for the opportunity to work in his group

DI Dr. Wolfgang Kandioller for his great support and supervision

Ao. Univ.-Prof. Dr. Vladimir Arion and Dipl.-Ing. (FH) Alexander Roller for X-ray data collection and structure refinement

The staff of the Core Facility for Mass Spectrometry and the Microanalytical Laboratory of the University of Vienna for the measurement of mass spectra and elemental analyses

My laboratory colleagues Christoph, Heiko and Barbara for their advice and for the pleasant work atmosphere

And my parents and family for their patience and for supporting me all these years

Abstract

Cancer is after cardiovascular diseases the second most leading cause of death worldwide and chemotherapy, often in combination with other therapies, is in many cases the choice of treatment. The transition metal complexes cisplatin and its derivatives oxaliplatin and carboplatin are one of the most common used anticancer drugs in chemotherapy. Due to the severe side effects (nephrotoxicity, neurotoxicity, etc.) and difficulties with acquired and intrinsic resistances, there is a great interest in the development of new anticancer drugs. One noteworthy candidate is the ruthenium complex IT-139, which has successfully completed phase I clinical trials with promising results. This compound shows high selectivity against tumor cells by selective accumulation in malignant tissue. In addition the compound is supposed to be reduced under the hypoxic conditions yielding the highly its highly reactive Ru(II) species. (“activation by reduction”). Due to the success of IT-139, Ru(II) complexes in addition to other noble metal organometallics such as osmium and rhodium sparked interest as potential anticancer agents. Especially complexes with the so-called “piano-stool” configuration offer promising potential for the development of novel metallodrugs due to their broad range of modification sites, allowing the fine-tuning of physico-chemical and biological properties.

The aim of this master thesis is the synthesis and characterization of novel half-sandwich complexes of ruthenium(II), osmium(II) and rhodium(III) employing *O*,*O* chelating 5-hydroxy-[1,4]-naphthoquinones as bioactive ligand scaffold. 5-Hydroxy -1,4-naphthoquinones such as juglone and plumbagin are secondary plant metabolites with a broad array of biological activities, including anti-inflammatory, antimicrobial and anticancer abilities. Their redox chemistry and the ability to generate reactive oxygen species offer interesting anticancer activity.

The synthesized complexes were characterized via X-ray diffraction analysis, elemental analysis, mass spectrometry and 1D/2D NMR spectroscopy. Additionally the redox properties were investigated by cyclic voltammetry, the solubility in aqueous solution was determined and the stability in aqueous medium was investigated by UV/Vis spectroscopy.

Zusammenfassung

Krebs ist nach kardiovaskulären Erkrankungen die zweithäufigste Todesursache weltweit und in vielen Fällen ist Chemotherapie, oftmals in Kombination mit anderen Therapieformen, die vielversprechendste Behandlungsmethode. Der Übergangsmetallkomplex Cisplatin und seine Derivate Oxaliplatin und Carboplatin sind einige der am häufigsten verwendeten Chemotherapeutika. Aufgrund ihrer schweren Nebenwirkungen (Nephrotoxizität, Neurotoxizität, etc.) und möglicher Probleme mit intrinsischen und erworbenen Resistenzen, besteht großes Interesse an der Entwicklung neuer Krebsmedikamente. Einer der nennenswertesten Kandidaten ist der Ruthenium(III) Komplex IT-139, der die Phase I der klinischen Studien mit vielversprechenden Ergebnissen abgeschlossen hat. Diese Verbindung zeigte hohe Selektivität gegenüber Tumorzellen durch die selektive Akkumulation in malignem Gewebe. Zusätzlich wird der Komplex vermutlich unter den sauerstoffarmen Bedingungen in Tumorzellen zur aktiveren Ru(II) Spezies reduziert ("activation by reduction"). Durch den Erfolg von IT-139 wurde auch das Interesse an organometallischen Verbindungen anderer Edelmetalle, wie Osmium und Rhodium, als potenzielle Chemotherapeutika geweckt. Besonders vielversprechend sind Komplexe mit der „piano-stool" Konfiguration, die durch ihre breite Modifikationsmöglichkeit eine Feinabstimmung der physikalisch-chemischen und biologischen Eigenschaften erlauben und somit großes Potenzial für die Entwicklung neuer Krebsmedikamente aufweisen.

Das Ziel dieser Masterarbeit ist die Synthese und Charakterisierung neuer Halbsandwichkomplexe von Ruthenium(II), Osmium(II) und Rhodium(III) unter Verwendung von 5-Hydroxy-[1,4]-naphthochinonen als zweizähnige *O*,*O* Liganden. 5-Hydroxy-[1,4]-naphthochinone wie Juglon und Plumbagin sind sekundäre Pflanzenstoffe die eine breit gefächerte Palette an biologischen Aktivitäten aufweisen, unter anderem entzündungshemmende und antimikrobielle Eigenschaften sowie Wirkung gegen Krebs.

Die hergestellten Komplexe wurden mittels Kristallstrukturanalyse, Elementaranalyse, Massenspektrometrie und 1D/2D NMR Spektroskopie charakterisiert. Zusätzlich wurde das Redoxpotential durch Cyclovoltammetrie, die Löslichkeit in wässriger Lösung, sowie die Stabilität in wässrigem Medium durch UV/Vis Spektroskopie untersucht.

Abbreviations

(M)Hz	(mega)hertz (s^{-1})
1D/ 2D NMR	one-/ two-dimensional NMR
Å	angstrom (10^{-10}m)
$CDCl_3$	deuterated chloroform
Cp^*	1,2,3,4,5-pentamethylcyclopentadienyl
cym	p-cymene
DCM	dichloro methane
DMSO	dimethyl sulfoxide
DMSO-d^6	deuterated dimethyl sulfoxide
DNA	deoxyribonucleic acid
eq	equivalent
EtoAc	ethyl acetate
EtOH	ethanol
g	gram
h	hour
HMBC	heteronuclear multiple bon correlation (NMR)
HR-MS	high resolution mass spectrometry
HSQC	heteronuclear single quantum coherence (NMR)
J	coupling constant (NMR)
MeOH	methanol
min	minute

MW	molecular weight
NMR	nuclear magnetic resonance
PBS	phosphate buffered saline
ppm	parts per million
r.t	room temperature
UV/Vis	ultraviolet/ visible
δ	chemical shift (NMR)

Table of Contents

Introduction

1.1 Cancer

Cancer is the second leading cause of death worldwide and is accountable for the decease of 8.8 million people in 2015, which makes it responsible for nearly 1 in 6 of all global deaths.[1] There were approximately 14 million new cases in 2012 and it is expected that the number will rise by about 70% over the next two decades.[2] Cancer has also an significant and increasing economic impact with globally costs of 107 billion US$ per year (2015) for cancer medication.[3]

In Austria nearly 39,000 people were newly diagnosed with malignant neoplasms in 2012 and one in four deaths was caused by cancer. The occurrence and types of cancer vary between men and women, also they differ significantly in their mortality rates (Fig. 1).[4] 2012 the most common cancer site in men was the prostate gland, and the most deaths were caused by lung cancer. In women breast cancer had the highest incidence rate and also the highest absolute number of deaths closely followed by lung cancer. The most deadly cancer site with the highest mortality rate in both sexes is the esophagus followed by the pancreas and the liver. [5]

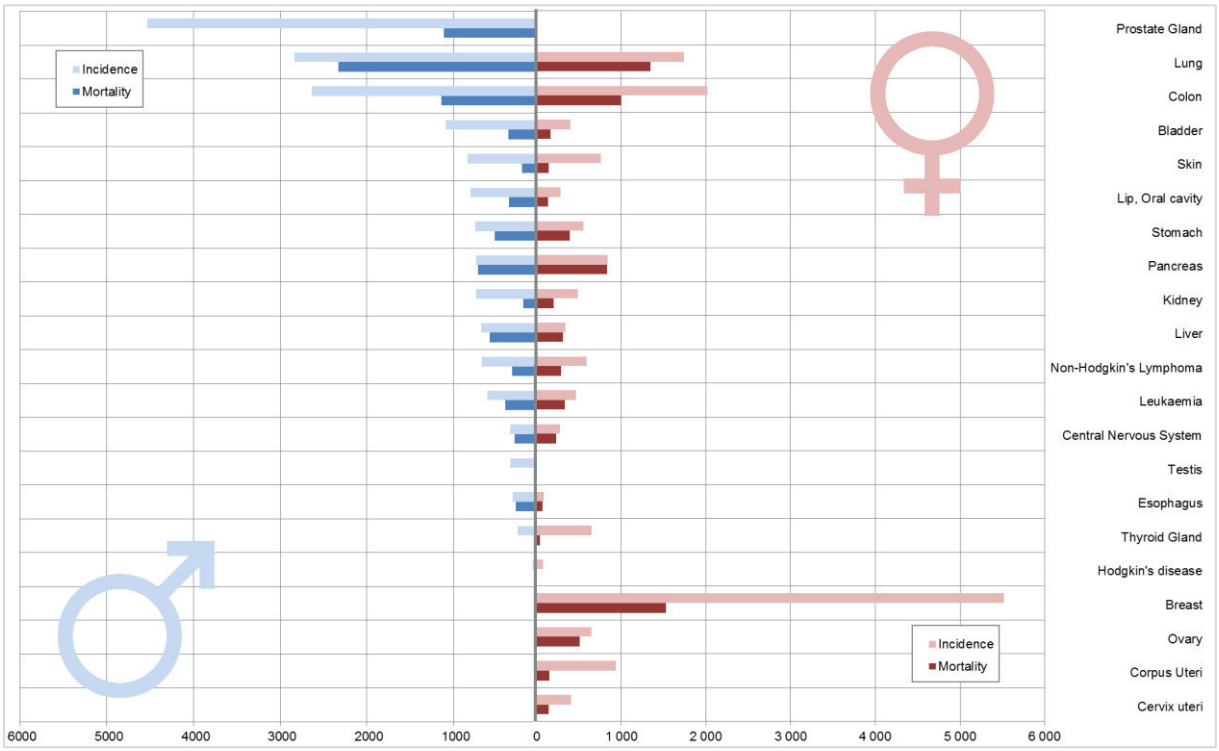

Figure 1: Absolute numbers of new cancer cases and deaths of different cancer sites in men and women (2012, Austria).[5]

1.2 Carcinogenesis

There tumors can be categorized in benign and malignant, both are the result of a transformation of normal healthy cells to tumor cells, called carcinogenesis. A benign tumor grows as a compact mass of cells, typically surrounded by a well-defined outer surface and only displaces and neither destroys nor invades surrounding tissue. However, it can turn into a malignant tumor with infiltrative and invasive growth, harming and destroying the surrounding tissue. Malignant tumor cells also have the ability to spread through the bloodstream and the lymphatic system to other body parts, a process called **metastasis**, which can result in the formation of secondary tumors. The carcinogenesis from normal cells to cancer cells can be divided into different phases (Fig. 2):

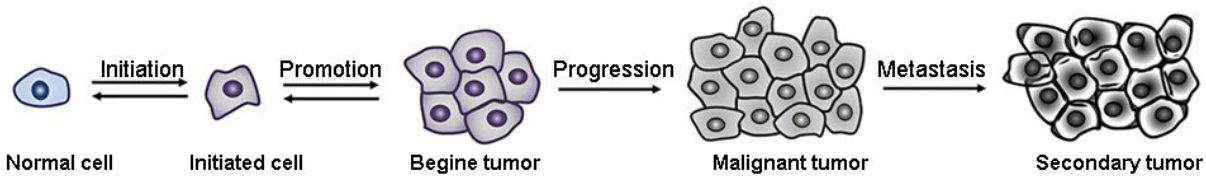

Figure 2: Transformation of normal cells into cancer cells [6]

During the **initiation phase**, a short time process, DNA gets damaged by cancer initiators like carcinogenic substances, reactive oxygen species (ROS), or UV and ionizing radiation. The normal cell turns into an initiated cell, unless the damage can be repaired or apoptosis gets triggered. The formed irreversible mutation is subsequently passed on to the daughter cells through cell division.

The result of the first phase is a cell population with identical mutations from the initiated cell through a raised mitosis rate and inhibited apoptosis. In contrary to the initiation phase the so called **promotion phase** is a long term process, where the cells need to be regularly affected by cancer promoters over a long period of time to promote proliferation of the initiated cells. In the case of too short or low exposure, the modifications in the cell may be repaired, which makes the promotion a reversible process.

The probability for additional mutations is increased, due to the higher proliferation rate in the promotion phase, and therefore more oncogenes are activated and more tumor suppressor genes are deactivated. The consequence is a very high proliferation rate and the irreversible transformation into a malignant cancer cell, a process called **progression phase**.[7]

Cancer cells differ from normal cells in many aspects and also vary from tumor to tumor. But all cancer cells share similar capabilities and characteristics[8], which lead to unrestricted growth and invasive behavior (Fig. 3).

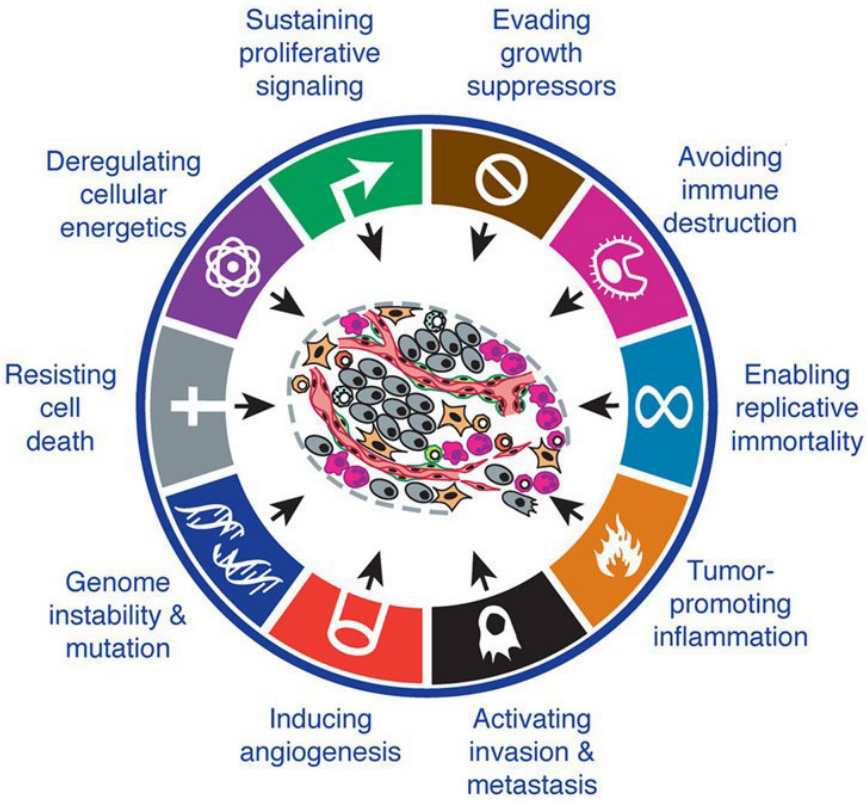

Figure 3: Capabilities and characteristics of cancer cells [8]

One of the most substantial traits of cancer cells is their **uncontrolled proliferation** caused by the deregulation of growth factor signals. In healthy cells the production and release of growth factors[9] is carefully balanced ensuring a constant number of cells and maintaining normal tissue architecture and function. In contrary cancer cells may produce growth factor ligands themselves, stimulate surrounding normal cells to provide the tumor with growth factors[10], elevating the levels of receptor proteins for growth factors on the cell surface, or alternate the structure of these receptors molecules to facilitate ligand independent signal transduction. Another important capability of cancer is the **evading of growth suppressors** like p53[11] and RB[12], which are key elements in the cellular regulatory circuits. The consequence is a constant cell division and proliferation of the tumor cells. Cancer cells also possess the ability of **resisting cell death,** probably gained by defects in the apoptosis (programmed cell death) inducing pathways[13]. The number of successive cell growth and division cycles is limited in most normal cells, directed by the shortening of the

telomeres. Cancer cells have the ability to extend the telomeric sequences in DNA[14], thus **enabling replicative immortality**. Due to the uncontrolled proliferation cancer cells have an increased metabolic demand, therefore needing more nutrients and ways to dispose metabolic waste. Another consequence is increased oxygen consumption, leading to hypoxia inside the tumor tissue. The formation of new blood vessels, the so-called **angiogenesis**[15] is induced by the upregulation of the vascular endothelial growth factor expression. A result of the accelerated formation is leakiness, restricted flow, also distorted and enlarged vessels[16], which altogether build the foundation of the EPR-effect[17] (enhanced permeability and retention). **Invasion and metastasis** are the characteristic traits of malignant tumors and typically start with development of alterations in the cell shape along with their attachment to other cells and the extracellular matrix. The next step is the invasion of local tissue followed by dissemination of single cancer cells from the tumor and their transport over blood vessels and/or the lymphatic system to distant organs and tissue. This whole process is called the invasion-metastasis cascade[18] and leads to the formation of micrometastases and finally to the growth of macroscopic secondary tumors. It is believed that cancer cells can gain the ability to **avoid immunological destruction** by T and B lymphocytes, macrophages and natural killer cells[8]. Another capability is the modification and reprogramming of the cellular metabolism to effectively support the uncontrolled proliferation. The multistep progression of carcinogenesis depends on a succession of gene alterations, and therefore **genome instability** favors the appearance of these required mutations. Cancer cells often accelerate the mutation rate [19] by increasing the sensitivity towards mutagenic agents, through breakdown of parts of the genomic maintenance and repairs systems. There is also evidence that in some cases tumor progression can be **promoted by inflammation** by supplying bioactive molecules to the cancer cells, like growth factors that sustain proliferative signaling, apoptosis limiting survival factors, and proangiogenic factors.[20]

1.3 Cancer treatment

The aim of cancer treatment is the removal of cancer while dealing the least amount of damage to the body as possible, or to prolong and increase the quality of the lives of the treated patients. Today there are many different forms of cancer treatment in use. The best choice of therapy is determined by the type of cancer, the location of the tumor, the stage of the cancer and the overall state of the patient. Usually a combination of different therapies is employed for the cancer treatment.[21]

Surgery is a form of cancer treatment in which the tumor is entirely or partially removed. In the case of invasive tumors and metastases only partially removal is possible and is usually accompanied by other forms of cancer treatment to eliminate the remaining tumor cells. **Radiation therapy** uses ionizing radiation like X-rays, gamma rays and charged particles to shrink tumors and destroy cancer cells, by directly damaging the DNA or by the creation of free radicals that also attack the genetic material inside the cells. **Immunotherapy** uses different methods to employ the immune system to fight the tumor by boosting the immune system or marking cancer cells. The **targeted therapy** interferes with the changes in cancer cells that help them to grow and survive. In **hormone therapy** the hormone-dependency of certain cancer types, like breast or prostate cancer, is used to inhibit the tumor growth. **Chemotherapy** uses anticancer drugs for the treatment of a wide variation of tumors by destroying cancer cells or stopping their growth. Chemotherapeutics are commonly used to reduce the tumor size before surgery or radiation therapy, to destroy cancer cells that may remain after other therapies, and also can eliminate reoccurring tumors or metastases. The goal of chemotherapy is to attack and eliminate the rapidly dividing cancer cells, but also normal cells, especially cells with a normally higher cell division rate, are affected ,which leads to a range of side effects like nausea, hair loss, heart and kidney problems, nerve damage and more.[22]

A broad range of chemotherapeutics is used in cancer treatment, which can be separated into several groups. There are drugs that act in more than one way and can therefore be assigned to more than one group by the way they induce apoptosis in cancer cells. Often different anticancer drugs are used simultaneously (combination chemotherapy) for an increased effectiveness of the treatment, due to potential synergistic effects and the possibility to avoid drug resistance.[23]

The main groups of anticancer drugs are:[24]

Alkylating agents

Alkylating agents can bind covalently to the nucleobases of the DNA. The formation of these bonds disrupts the replication and transcription of the DNA and therefore inducing apoptosis.

Antimetabolites

Antimetabolites interfere with the synthesis of DNA. These drugs damage cells only during the S phase and are typically analogues of pyrimidine, purine or folic acid.

Anti-tumor antibiotics

Most prominent representatives are anthracyclines, originally derived from the fungus *Streptomyces*.

Mitotic inhibitors

Mitotic inhibitors prevent cancer cells from completing mitosis in the M phase of the cell cycle by disrupting microtubule polymerization. These drugs are often derived from natural products like plant alkaloids and other compounds.

Topoisomerase inhibitors

These drugs interfere with topoisomerase enzymes, which unwind DNA double strands during replication and transcription. The interruption of this function induces breaks in the chromosomal DNA leading to apoptosis.

Hormonal therapy

Hormone-like drugs inhibit the production or activity of specific cancer growth related hormones, leading to a cease in growth or cell death in certain types of cancer.

1.4 Metal-based drugs in medicine

Metals are required for performing necessary life functions. The four metals Ca, K, Mg, Na are considered essential bulk elements, whereas the transition metals Co, Cr, Cu, Fe, Mn, Mo, V, Zn are regarded as essential trace elements. They are necessary in a broad array of biochemical processes playing structural and functional roles and as electrolytes. Inadequate intake of these elements can result in deficiency symptoms and diseases, while in the other hand an excessive intake can cause severe side effects. The chronic exposure of other metals, especially so-called heavy metals like Hg and Pb, through food or the environment leads to the accumulation of these elements in the soft tissue and inducing serious damage to the body.

Metal-based drugs have proven themselves in clinical use for diagnosis and treatment of various diseases, being an interesting and promising research field.

One application is the use as contrast agents for magnetic resonance imaging (MRI). Paramagnetic complexes of Gd(III), Fe(III) and Mn(II) are used as contrast agents, due to their ability to change the relaxation properties of the surrounding H_2O molecules, resulting in an improved imaging contrast .[25] Complexes of the radionuclides ^{99m}Tc and ^{68}Ga are utilized as radioisotope agents in diagnostic nuclear medicine.[25-26] Depending on the attached ligand scaffold, they are able to bind and accumulate in certain types of tissue. The distribution in the body can be determined by measuring the radioactive emission of the utilized radioisotopes via single-photon emission computed tomography (SPECT) or positron emission tomography (PET).

Another application of metals is in the treatment of various diseases. Gold complexes are used for the treatment of rheumatoid arthritis or lithium salts as antidepressant. One potential application field is the application of metal based drugs as chemotherapeutics in cancer treatment and numerous metal complexes based on Au, Ga, Ir, Pt, Rh, Ru, Ti and Os have been shown to exhibit antineoplastic abilities.[25]

1.4.1 Platinum-based anticancer drugs

The cytotoxic potential of *cis*-diamminedichloridoplatinum(II) (Fig. 4) was serendipitously discovered by B. Rosenberg in the 1960s.[27] Cisplatin was proven to be highly active against bladder, testicular, ovarian and lung carcinoma and was approved for clinical use in in 1978.[28] There are also two other worldwide clinically established anticancer platinum(II) complexes namely carboplatin and oxaliplatin (Fig. 4). Platinum-based drugs are used in about 50% of all tumor therapies.[29]

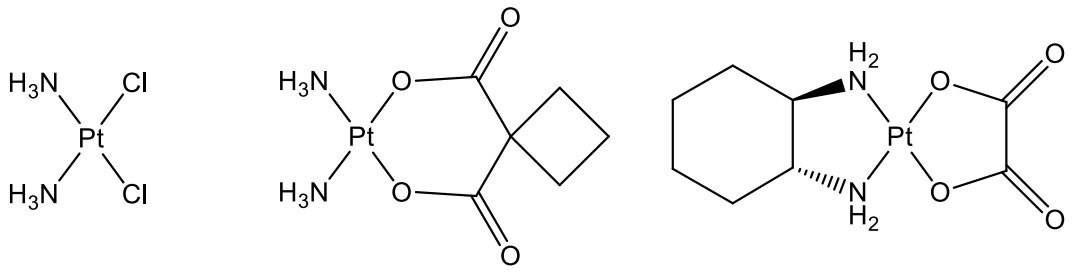

Figure 4: Structures of cisplatin (left), carboplatin (middle) and oxaliplatin (right)

These three compounds are complexes with a square planar geometry but differ in their leaving group and am(m)ine ligand composition. The replacement of the chlorido leaving groups by the bidentate cyclobutanodicarboxylato ligand led to the development of carboplatin. This modification resulted in a more inert complex and therefore a decreased toxicity and disposal of nephrotoxicity, followed by increased stability and better water solubility. Oxaliplatin is the result of a shift to a bidentate oxalate leaving group and an introduction of a chelating 1,2-diammino-cyclohexane ligand leading to a complex with a slightly different activity profile, especially its effectiveness against metastatic colorectal cancer which are cisplatin resistant.[28]

After the intravenous administration of cisplatin, the complex can enter cells via passive diffusion or assisted by copper transporters.[30] The activation of cisplatin by aquation is strongly dependent on the chloride concentration. The low intracellular chloride concentration (4 mM) facilitates hydrolysis (Fig. 5). The formed aqua complex is able to react with bionucleophiles such as nucleobases. The metal center coordinates to the N7 atom of the purines, preferably guanine, in the DNA leading to the formation of different cisplatin-DNA adducts. The generated adducts consists of 65% intrastrand crosslinks between neighboring guanine bases, followed by 25% intrastrand crosslinks between guanine and adenine, and a small portion of

interstrand crosslinks and protein-DNA link products.[28] The result is interference with mitosis and transcription, ultimately leading to apoptosis of the cell.

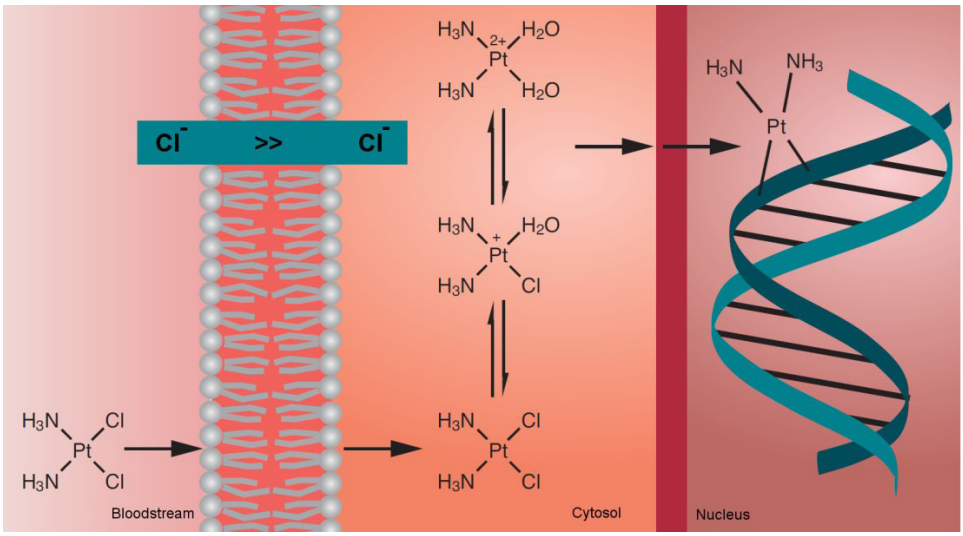

Figure 5: Formation of the active aqua species and binding to DNA of cisplatin[28]

However, most of the administered cisplatin binds to proteins and other biomolecules, especially to S-donors like glutathione[31] which deactivates the metallodrug. As a consequence only 1% of the administered drug dose interacts with DNA. Fast proliferating cells, like tumor cells, are most affected by cisplatin, but normal cells are also impaired, leading to various severe side effects like nephrotoxicity, neurotoxicity, ototoxicity and nausea. Furthermore tumor cells can develop resistance against certain platinum compounds, which encourages the research and development of novel platinum based agents like platinum(IV) complexes, with potential properties like reduced side effects, oral administration, overcoming of resistance and activation by reduction to platinum(II)[32], and other anticancer drugs with different metal centers.

1.4.2 Ruthenium complexes

On the search for novel anticancer metal complexes with different activity profiles, lower side effects and novel modes of action, ruthenium compounds have emerged as promising candidates. Their preferred six-coordinated octahedral configuration provides a broader spectrum of modification, which enables fine-tuning of steric and electronic properties and also an expended variety of ligands. A substantial benefit of ruthenium based anticancer drugs is the lesser toxicity, which is in part attributed to the similarity of ruthenium to iron. Another cause for the general lower toxicity of some ruthenium-complexes could be the “activation-by-reduction” mechanism.[33] Under physiological conditions three relevant oxidation states: +II, +III, (+IV, generally unstable[34]) are accessible for ruthenium. Complexes of Ru(III) are more inert toward ligand exchange reactions than the respective Ru(II) species. The main principle behind “activation by reduction” is the possible reduction of Ru(III) to the kinetically more active Ru(II),facilitated under the reductive microenvironment present within tumor tissue.[35] This reductive conditions are caused by inadequate formation of new blood vessels and therefore increased anaerobic metabolism of cancer cells yielding hypoxic conditions.

The first ruthenium based anticancer drug completing phase I clinical trials was [ImH][trans-$RuCl_4$(DMSO)(Im)] called NAMI-A (Fig. 6). This octahedral Ru(III) complex, with axial imidazole and DMSO ligands and four equatorial chlorides, showed low cytotoxicity towards cancer cells *in vitro*, but significant efficacy against metastases *in vivo*.[36] Because of low therapeutic efficiency and disease progression, further clinical investigations of NAMI-A were terminated.[37]

Another Ru(III) complex, finishing clinical Phase I trials[38] was (InH)[trans-$RuCl_4(In)_2$] called KP1019, with two axial indazole ligands and four chlorides in equatorial position (Fig. 6). Due to limited solubility, KP1019 was replaced by its sodium salt analogue IT-139 (former name NKP-1339), which also successfully completed clinical phase I/IIa studies I with promising results against solid tumors like non-small cell lung cancer, colorectal carcinoma and gastrointestinal neuroendocrine tumors.[39] The increased water solubility of IT-139 compared to KP1019 allows administration of larger doses. The very limited side effects are a major advantage of this class of ruthenium based drugs compared to other chemotherapeutics.

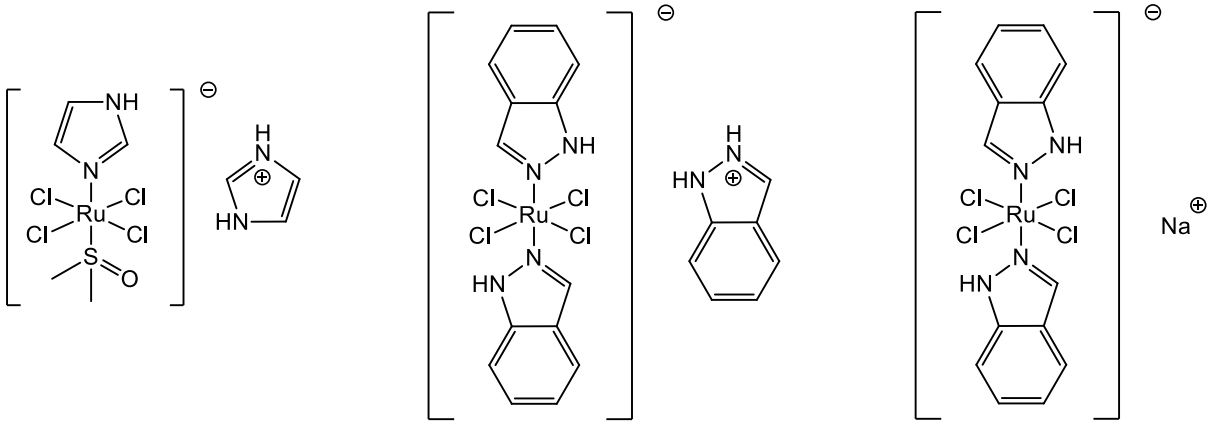

Figure 6: Structures of NAMI-A (left), KP1019 (middle) and IT-139 (right)

IT-139 is administered intravenously and shows strong affinity to serum proteins and binds fast to albumin and transferrin.[40] It binds preferably to albumin, which is exploited as a transport and delivery system and also for tumor targeting, because albumin accumulates in malignant tumor tissues due to leaky blood capillaries combined with the absence of lymphatic drainage (EPR-effect).[41] IT-139 is not reduced effectively while bound to serum proteins,[42] therefore activation of the complex by reduction takes place inside the cancer cell, after the release of the drug from the protein. There is a rise in evidence for an anticancer activity of IT-139, not based on direct DNA damage.[43] The involved mechanism suspected for the cytotoxicity are targeting the chaperon protein GRP78[40] (a key factor of the unfolded protein response), endoplasmic reticulum (ER) stress[44] and the generation of reactive oxygen species (ROS) leading to oxidative stress, thereby inducing apoptosis of tumor cells via the mitochondrial pathway[45]; and the arrest of the cell cycle in G_2/M phase[46].

One emerging class of ruthenium based metallodrugs are Ru(II)-arene complexes of the general form [(η^6-arene)Ru(X)(Y)(Z)], where X is a leaving group and Y/Z are two mono- or one bidentate ligand. These half-sandwich complexes adopt the so-called "piano-stool" configuration, named by their structural resemblance to a piano stool, where the arene represents the seat and the three remaining ligands the feet. (Fig. 7)

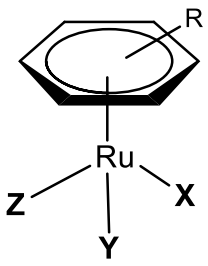

Figure 7: Ru(II) arene complex with piano stool configuration

The first promising candidates of this compound class were RM175 with a bidentate ethylenediamine ligand (Fig. 8) and RAPTA-C featuring three monodentate ligands, one being pta (1,3,5-triaza-7-phospoadamantane). RAPTA-C exhibit low cytotoxicity *in vitro*, but remarkable antitumor properties *in vivo* like high selectivity and antimetastatic activity similar to NAMI-A.[47]

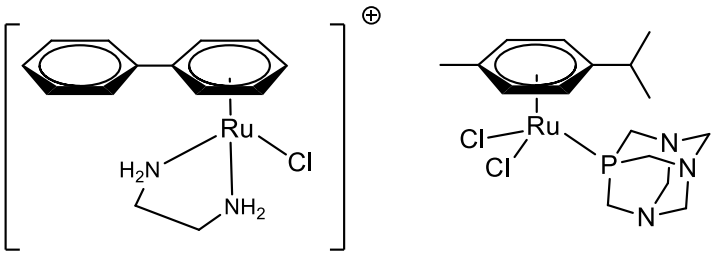

Figure 8: Structures of RMI175 (left) and RAPTA-C (right)

This class of half-sandwich complexes provides numerous possibilities for modification of the coordination sphere and therefore a broad spectrum of attainable properties. The arene offers synthetic diversity and opportunities of derivatization, making it an outstanding scaffold for targeted chemotherapy through the coupling of

organic fragments.[48] Bi- and monodentate ligands with additional functionalities or biologically activity itself can be introduced, allowing fine-tuning of biological and physico-chemical properties. One key trait is the hydrolysis rate of the leaving group, yielding the highly reactive aqua complexes. Due to the high extracellular chloride concentrations (100 mM), the less reactive chlorido complexes are predominantly found in the blood plasma. However, the chloride concentration is distinctly lower inside the cell nucleus (4 mM), facilitating the hydrolysis or the Ru-Cl bond.[49] Another great feature are the amphiphilic properties arising by the hydrophilic metal center and hydrophobic coordinated arene, thereby influencing cellular uptake. This versatility is essential to allow the complex to reach and react with the intended target site. It is proposed that the anticancer activity of Ru(II)-arene complexes may only be partly related to DNA interactions[50]. Instead inhibition of protein kinases, topoisomerases, carbonic anhydrases and alterations in the redox balance of cancer cells by the metal complexes was reported.[51] Changing the redox balance can disturb the oxidant-antioxidant balance in favor of an oxidizing environment inside the cell and potentially leading to generation of ROS and subsequently oxidative stress. The resulting cell damages like single-strand breaks in DNA, disruption of the mitochondrial inner membrane, lipid peroxidation causing disturbed cell membranes, changes in secondary protein structure by oxidation of the cysteine residue can lead to apoptosis.[52] Because cancer cells have an already elevated level of reactive oxygen species, they are more sensitive to oxidative stress than healthy cells, therefore providing a potential starting point for cancer treatment.

The choice of chelating ligand is an important factor for rate of hydrolysis, cytotoxicity and stability. There is various research ongoing on several types of chelating systems for Ru(II)-arene complexes with different coordination motifs such as N,N-, N,O-,S,O- and O,O-donor sets.

1.4.3 Osmium complexes

Compounds of the heavier congener osmium attracted interest due to the observed anticancer potential of ruthenium complexes.[53] Besides their close proximity, osmium exhibits several features distinct from ruthenium like their increased inertness to ligand substitution, preference for higher oxidation states and sufficient stability under physiological conditions. Similar to their ruthenium analogues, Os(II)-arene complexes demonstrated cancer cell cytotoxicity comparable to cisplatin.[54] These compounds also adopt the “piano stool” configuration and feature the advantages of this compound class, like fine-tuning of complex properties and thereby influencing the biological activity of the drugs. Also osmium complexes with the oxidation state +III and +IV have shown anticancer ability and are currently under research.[53]

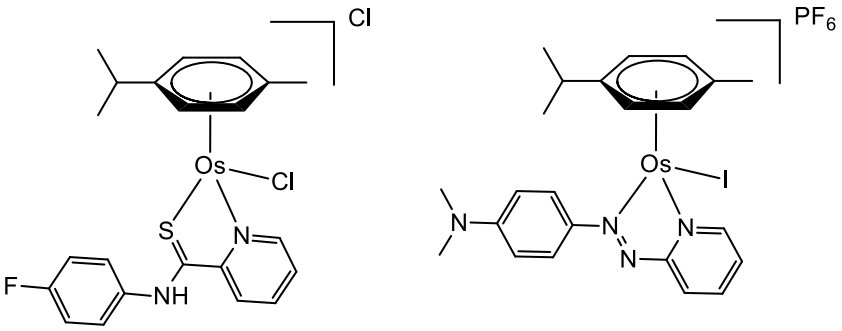

Fig. 9: Examples of anticancer Os(II) compounds: complex employing 2-pyridinecarbothioamides (left), FY026 (right)

1.4.4 Rhodium complexes

Another interesting transition in the field of organometallic anticancer drugs is rhodium. Although first mentioned antitumor properties for a rhodium compound ($RhCl_3x3H_2O$) were published in 1953[55], rhodium complexes just recently received broader attention as potential anticancer drugs. The initial lack of interest can be attributed to the kinetic inertness, low solubility and in some cases a high overall toxicity.[56] This inertness can be overcome by the facial coordination of arene ligands and Rh(III) complexes bearing anionic 1,2,3,4,5-pentamethylcyclopentadienyl (Cp^*) ligand have been studied for their anticancer potential. Compared to neutral arene ligands, the coordination of the Cp^* ligand leads to an even stronger *trans* effect, increasing the hydrolysis rates by several orders of magnitudes.[57]

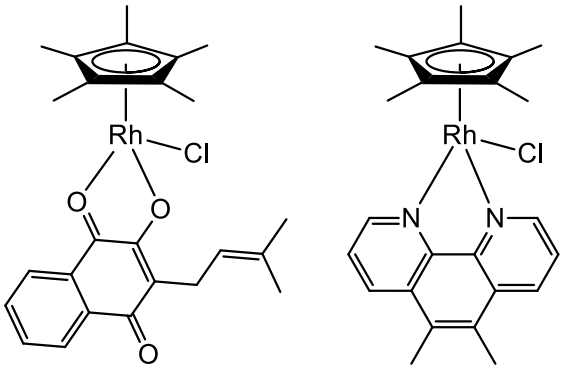

Figure 10: Examples of Rh(III)-arene complexes with 1,2,3,4,5-pentamethylcyclopentadienyl (Cp^*) employing lapachol (left) and 5,6-dimethylphenanthroline (right).

1.5 [1,4]-Naphthoquinones

1,4-Naphthoquinones are quite common in nature and are found in plants, animals and microorganisms, where they play a vital role in electron transfer processes, especially in the biochemistry of energy production like the respiratory chain and photosynthesis. One prominent representative of 1,4-napthoquinones, Vitamin K_1 (Fig. 11) has an important role as an electron acceptor in photosynthesis and also acts as the precursor for most derivatives of the vitamin K group, which are essential cofactors in different carboxylases in mammals. In general 1,4-naphthoquinones display various biological activities such as antiallergic, antibacterial, antifungal, anti-inflammatory, antiviral, antithrombotic and anticancer activity, therefore being the center of research for several types of drugs.[58] Besides various other naphthoquinone containing potential antitumor drugs, there are two interesting 1,4-naphthoquinone compounds Cpd 5 and NSC 95397 (Fig. 11) with anticancer ability, both inhibiting CDC25 phosphatase, an essential cell cycle regulator, controlling the transition of cells by dephosphorylation of cyclin-dependent kinases.[59]

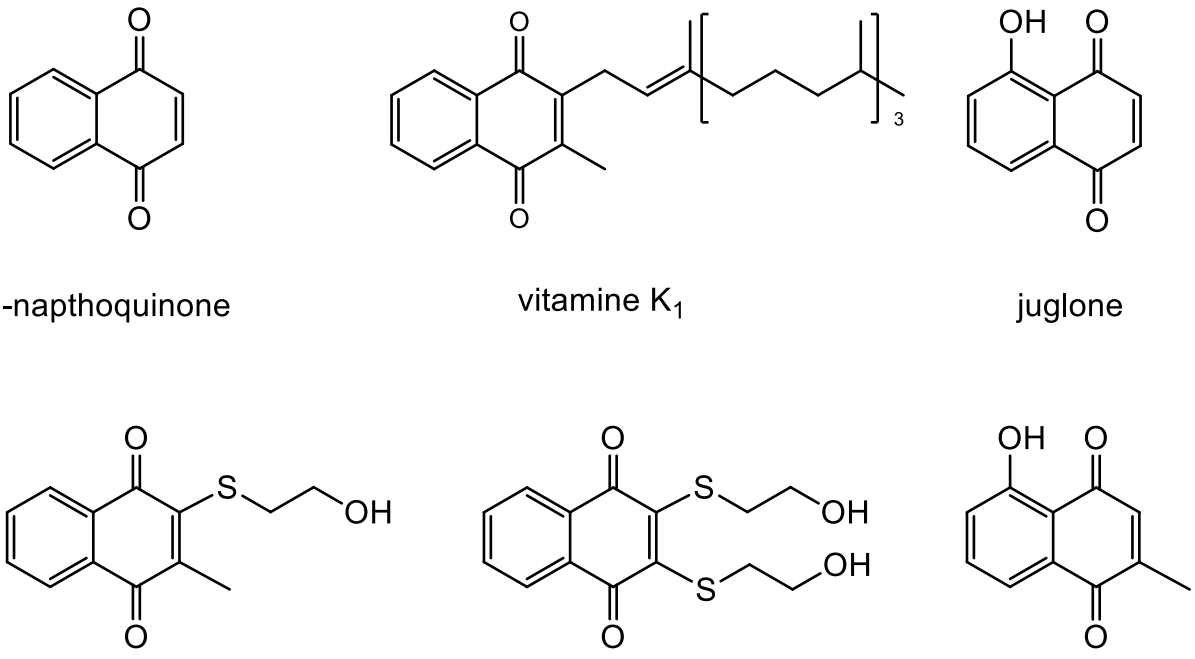

Figure. 11: Structures of important 1,4-naptoquinones

The -5-hydroxy -1,4-naphthoquinones juglone and plumbagin (Fig. 11) are secondary plant metabolites occurring predominantly in the family *Juglandaceae,* especially in the walnut tree *Juglans*, and the family *Plumbaginaceae.* Both compounds have been used in traditional folk medicine for the treatment of several different health conditions, ranging from elimination of internal parasites and rheumatic pain to therapy of bacterial, viral, fungal infections and many more. Both molecules have sparked interest as potential anticancer drugs due to their biological activity. Juglone has demonstrated the ability to interfere with mitosis progression by inactivating for mitosis essential cysteine rich proteins,[60] and can induce apoptosis through a mitochondrial pathway mediated by the generation of ROS.[61] Plumbagin has an immense range of biological activities, starting from antimicrobial[62], antimalarial[63], anti-inflammatory[64] to immunosuppressive[65], neuroprotective[66] and anticancer abilities. The observed effects against tumor cells emerge through multiple signaling pathways. The mechanisms for the anticancer activity were primarily related to inducing apoptosis, cell cycle arrest, autophagy and also inhibition of invasion, migration and angiogenesis.[67] Plumbagin was shown to be an inhibitor of DNA topoisomerase II[68] and also inhibits mitosis by disrupting the microtubule network[69]. Most of these reported anticancer activities are based on the generation of oxidative stress. Structure–activity relationship (SAR) studies revealed that the hydroxyl group at position 5 plays an essential part for increased cytotoxicity compared to other 1,4-naphthoquinones.[70]

Due to their structure, 1,4-naphthoquinones are excellent producers of reactive oxygen species (ROS). The underlying reaction is a cyclic process of a 2 electron reduction of the naphthoquinone to the hydronaphthoquinone or a 1 electron reduction to a seminaphthoquinone radical (Fig. 12), followed by the (auto)oxidation back to the naphthoquinone.[58]

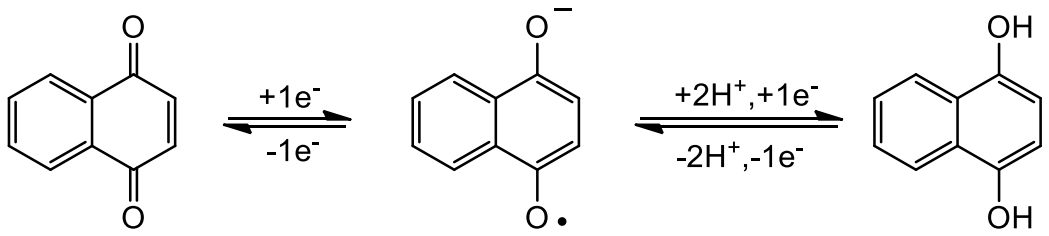

Figure 12: Structures of naphthoquinone (left), seminaphthoquinone radical (middle) and hydronaphthoquinone (right)

During the oxidation of the seminaphthoquinone radical back to the naphthoquinone, oxygen can be reduced forming a superoxide radical anion, which is the precursor of most other reactive oxygen species.[71] Furthermore 1,4-naphthoquinones can react with biological nucleophiles like thiols and amines at a free C-3 or C-2 position via Michael addition. For example biomolecule the cysteine residue of glutathione can form such adducts, leading to additional oxidative stress in cells.[72] Also intercalation into the DNA by plumbagin and other naphthoquinones was reported.[73]

2 Results and Discussion

The goal of this master thesis was the synthesis of novel half-sandwich complexes with ruthenium(II), osmium(II) and rhodium(III) as metal center bearing different *O*,*O* chelating 5-hydroxy-[1,4]-naphthoquinones as bioactive ligand scaffolds and chloride or imidazole derivatives as leaving groups.

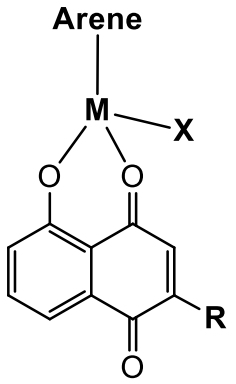

Arene = p-cymene, Cp*

M= Ru^{II},Os^{II},Rh^{III}

X= Cl,1-methylimidazole, imidazole

R= H,CH_3, NH-Ph

The synthesized complexes were characterized via, elemental analysis, mass spectrometry, 1D/2D NMR spectroscopy and where possible by X-ray diffraction analysis. Additionally the redox chemistry was investigated by cyclic voltammetry and the behavior in aqueous solution was determined by UV/Vis spectroscopy.

2.1 Synthetic scheme

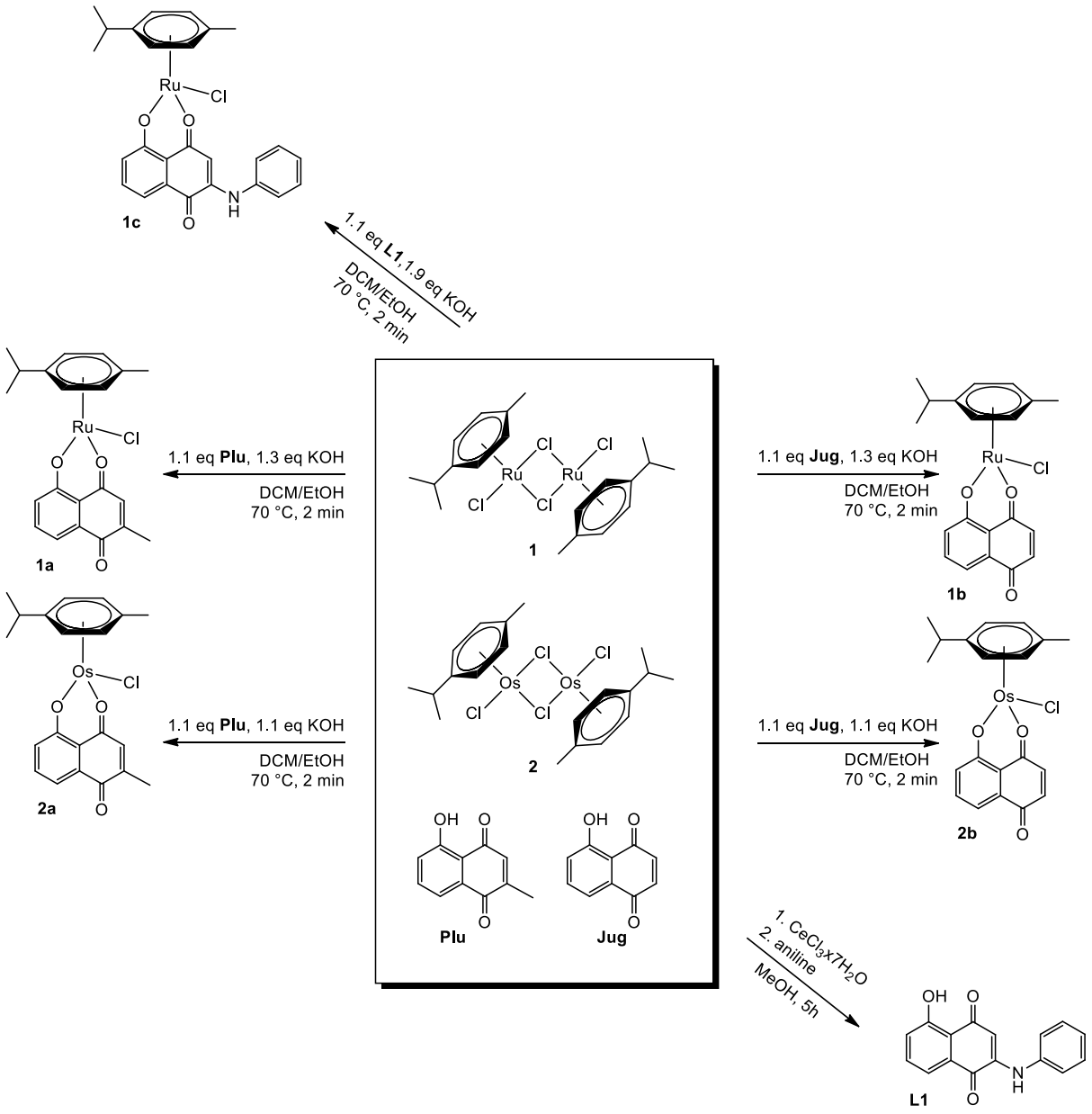

2.2 Synthesis and characterization of the ligand

Besides juglone and plumbagin there was also an interest in other 5-hydroxy-[1,4]-naphthoquinones, especially nitrogen derivatives. Two problems arose for the synthesis of nitrogen derivatives starting from juglone. Firstly only mono-amino derivatives can be obtained with non-cyclic amines, secondly a regioselective reaction is needed to avoid an elaborate isolation of the mono-amine compounds. With the use of $CeCl_3 \cdot 7H_2O$ as a catalyst in combination with ultrasound as energy source, a regioselective addition of aniline in position 2 to form 2-(aniline)-5-hydroxy-[1,4]-naphthoquinone with good yield and no byproducts is possible.[74] The reaction was performed accordingly yielding the desired mono-substituted juglone in moderate yield (55%).

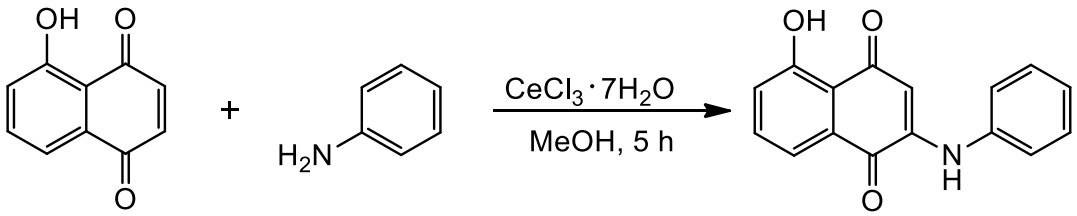

L1

NMR

All ^{1}H-NMR, ^{13}C-NMR, and 2D spectra of the ligand were measured in DMSO-d_6 and the detected signals were assigned by evaluation of the 2D-NMR spectra.

1H-NMR

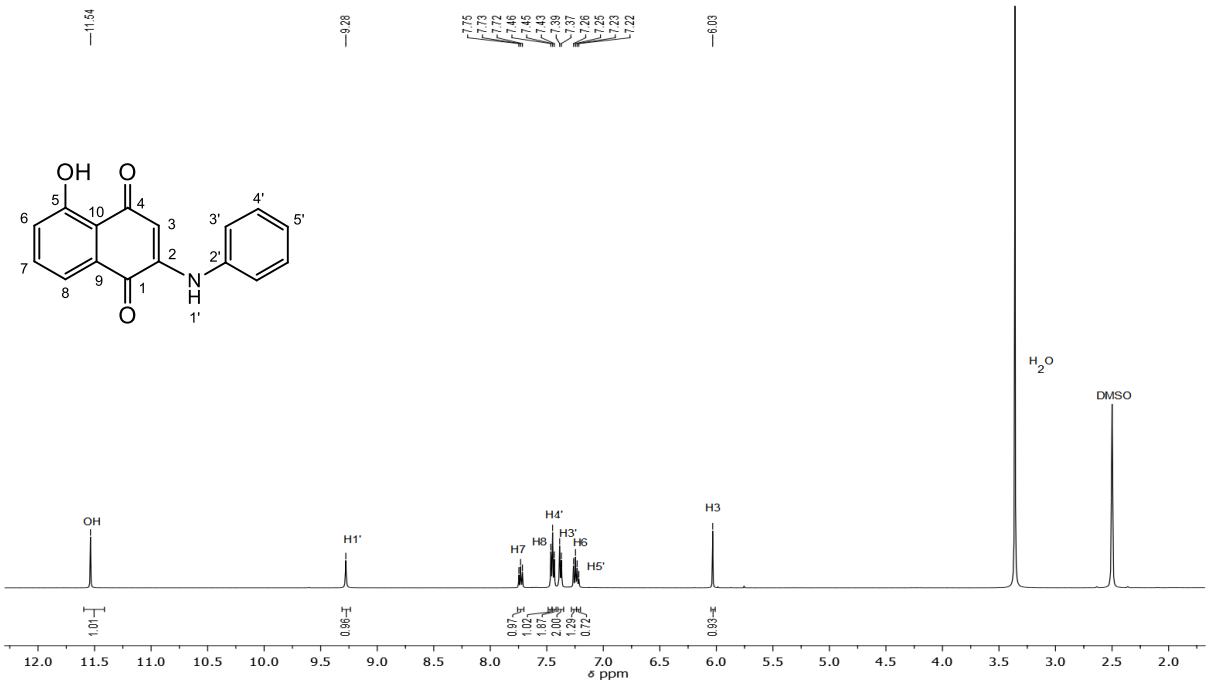

Figure 13: ^{1}H-NMR of **L1**

In comparison to juglone all proton signals are slightly shifted upfield with the exception of H7. The H2 signal disappeared due to the reaction with aniline and the signal of H3 is shifted upfield by 0.9 ppm. The NH signal of the amine is found at around 9.3 ppm, also the aromatic signals of the naphthoquinone and the phenyl rest overlap partially between 7.0 -7.5 ppm. The absence of a H2 signal confirms the regioselective reaction only yielding the desired 2-(aniline)-5-hydroxy-[1,4]-naphthoquinone.

^{13}C-NMR

The carbonyl signal of C4 was found at 181 ppm, slightly shifted upfield by 9 ppm, while C1 showed only a negligible upfield shift compared to juglone. The aniline substitution affects the signal of C2 with a downfield shift of 8 ppm, whereas C3 is found at 102 ppm, shifted upfield by 36 ppm in comparison to the signal of the precursor at 138 ppm. All other carbon signals presented only a slightly upfield shift.

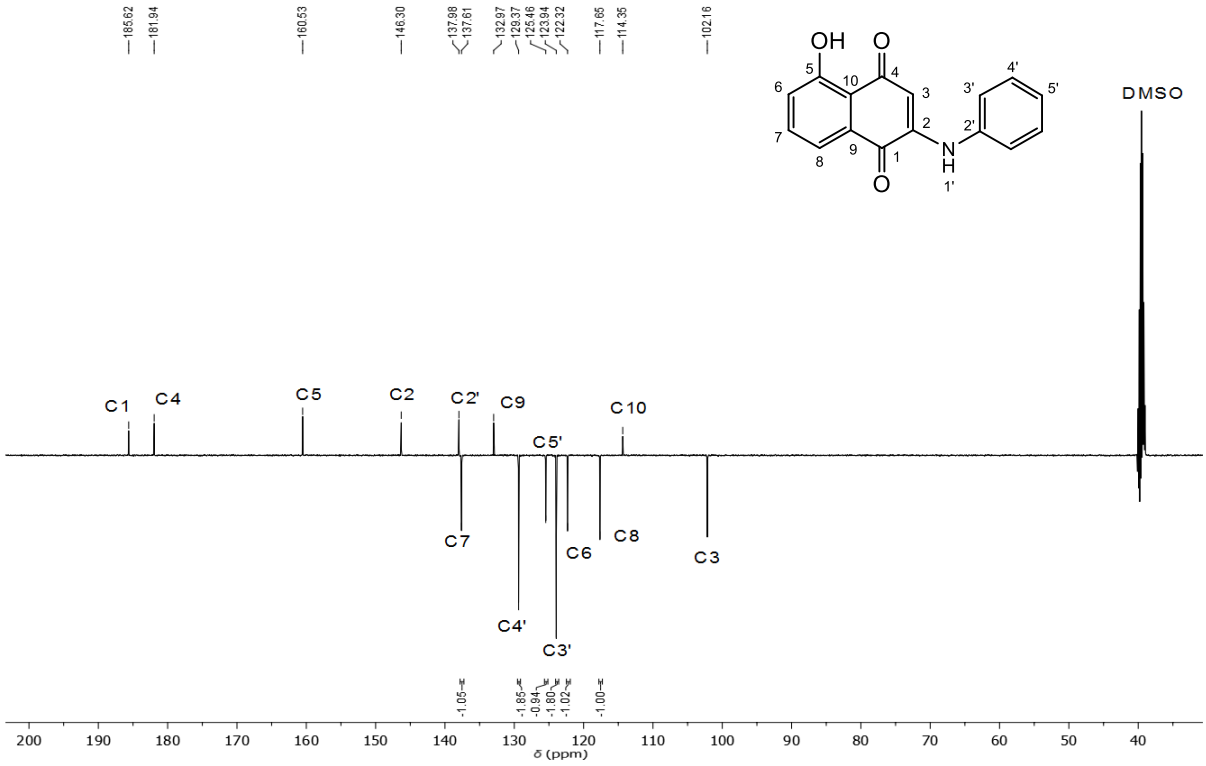

Figure 14: ^{13}C-NMR of **L1**

2.3 Synthesis and characterization of the complexes

In general the dimeric precursor $[M(p\text{-cymene})Cl_2]_2$ of either ruthenium or osmium were reacted with a slight excess of the respective 5-hydroxy-[1,4]-naphthoquinone (1.0 eq) under microwave-assisted conditions at 70 °C. Purification of the reaction mixture afforded the products in moderate to excellent yields (57-97%).

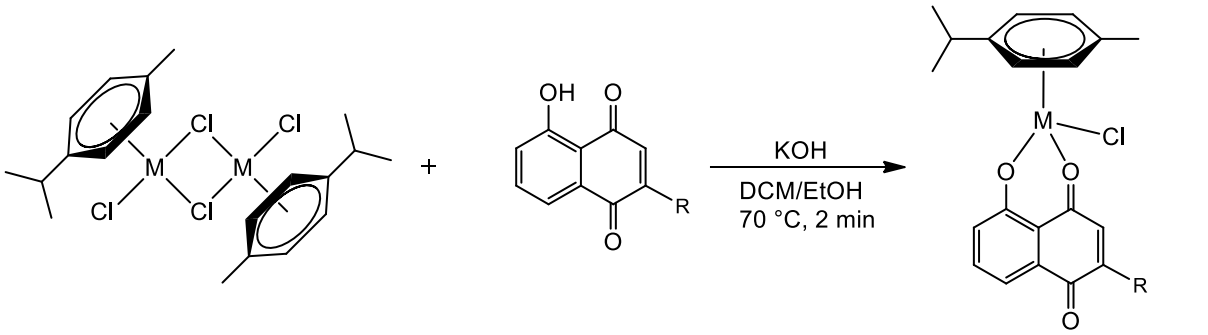

1 a-c, 2a-b

R = H, CH_3, NH-Ph
M = Ru^{II}/Os^{II}

The great challenge for obtaining this kind of complexes was reaching complete conversion, because there was no satisfactory method found to separate the products from the respective dimeric precursors. The conversion rate was monitored by ^1H NMR, evaluating the protons of the p-cymene ligand, due to a observable shift upon coordination of the 5-hydroxy-[1,4]-naphthoquinones. The addition of a larger excess than 0.1 eq. of the ligand to shift the reaction equilibrium in favor of the product led to a decrease in conversion. An interesting observation is the big role of the addition order of the reactants during the reaction. A combination of dimeric precursor and ligand followed by addition of the base, or the complex accompanied by the base and subsequent adding of the ligand, both resulted in formation of the desired product. At the same time all reactions where the 5-hydroxy-[1,4]-naphthoquinone was deprotonated before treatment with the dimeric precursor, afforded no product at all. Also other deprotonating agents were checked, but never showed nearly as good results as KOH. Another essential detail is the use of EtOH (96%), since all reactions with dry solvents exhibited a decreased conversion. While the synthesis of the ruthenium compounds also were achieved by stirring the reaction mixture at room temperature for 40 h, the osmium compounds never reached full conversion without microwave assistance. Also small changes in temperature,

duration and amount of power used during the microwave reactions had great impact on conversion.

NMR

All ^{1}H-NMR, ^{13}C-NMR, and 2D spectra of the ruthenium and osmium compounds were measured in $CDCl_3$, due to the limited stability in DMSO-d_6. The detected signals were assigned via 2D-NMR analysis.

^{1}H-NMR

The coordination affects the cymene signals of the ruthenium complexes with a slightly downfield shift compared to the dimeric precursor. Only exception is the signal of Hc with a slightly upfield shift. The doublet of Hd changed to a doublet of doublets and Hg changed from duplet to triplet.

Cymene signals of the osmium complexes were also shifted downfield to some extend compared to the precursor, except the signal of Hc and Hd which were shifted upfield by about 0.2 ppm. The doublet of Hd and Hc changed to a doublet doublets (Hd) and a triplet (Hc), while Hg changed from a doublet to triplet.

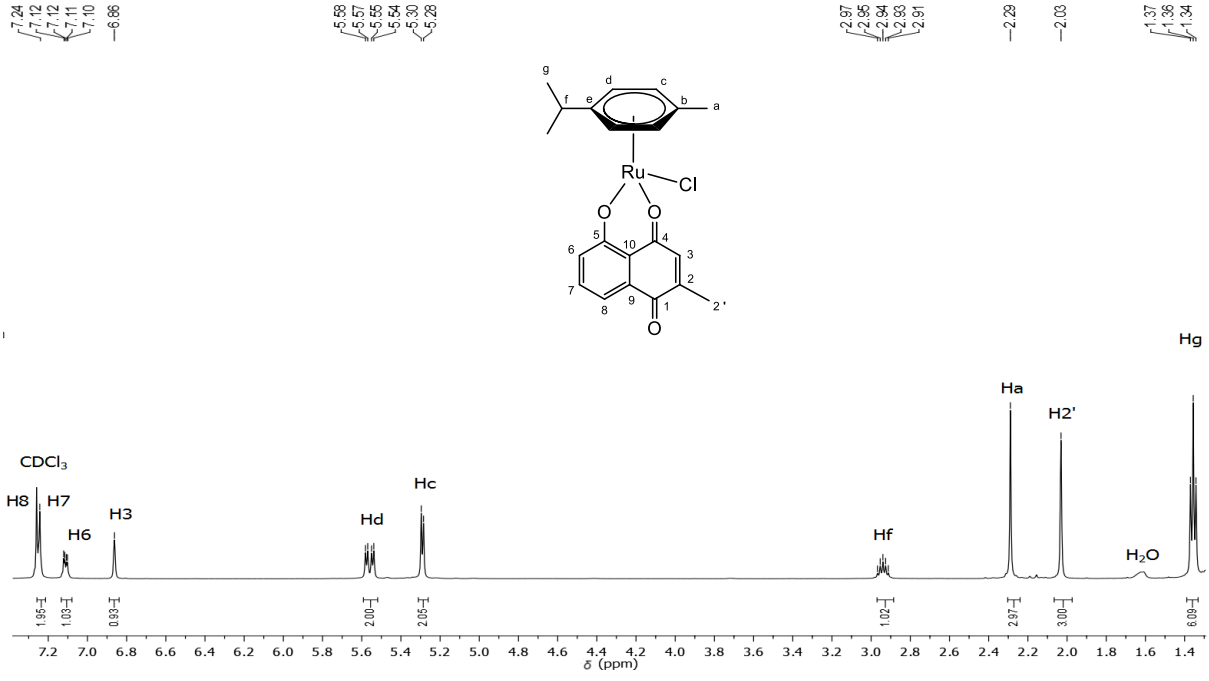

Figure 15: ^{1}H-NMR of **1a**

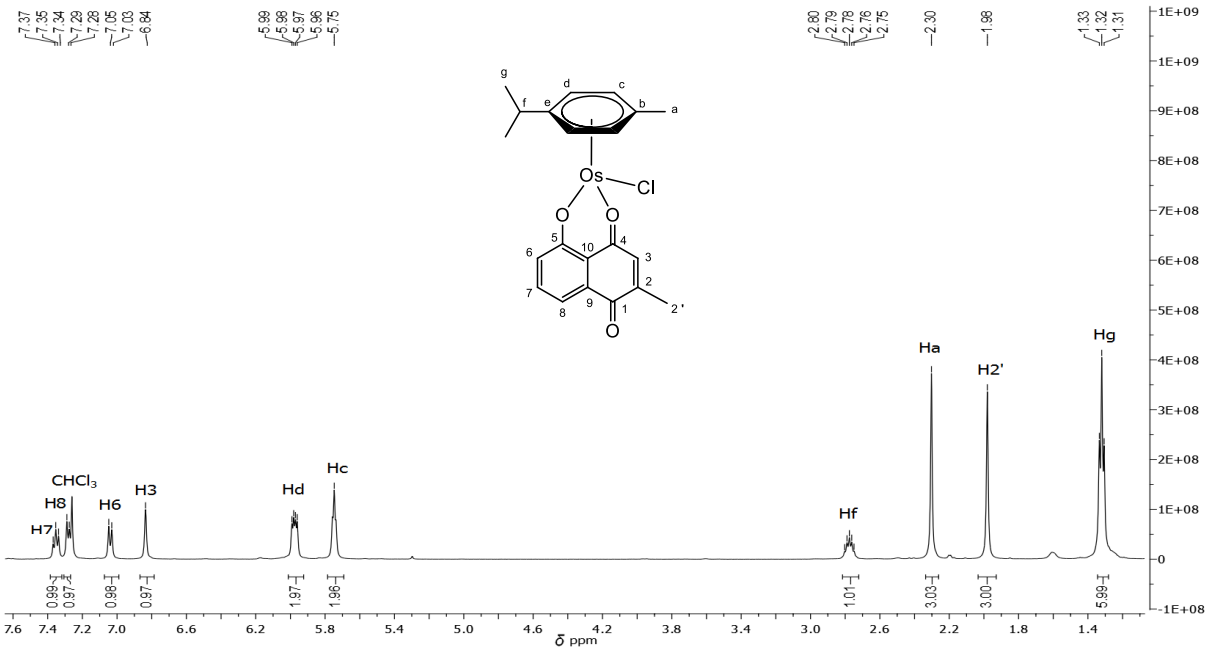

Figure 16: ^{1}H-NMR of **2a**

The coordination of ruthenium or osmium caused an upfield shift of the respective coordinated 5-hydroxy-[1,4]-naphthoquinone signals by 0.3–0.35 ppm, with exception of a slight downfield shift of H3. Also the OH signal (usually around 12 ppm) vanished confirming coordination to the metal center. In the case of the plumbagin complexes, the signals of H8 and H7 were completely or partially overlapped with the $CHCl_3$ signal. For the osmium complexes the signal of H7 is shifted more downfield than the H8 signal, while for the ruthenium complexes it is vice versa.

^{13}C-NMR

Overall the signals of p-cymene were found more or less at the same chemical shift as occurring in the respective precursor.

The ruthenium coordination inducing an upfield shift of the carbonyl signal C4 and f the neighboring C3 by 7.5 ppm and 2 ppm, respectively. In contrast the C5 and the nearby C6 are shifted down field by 8.5 ppm and 8.3 ppm, respectively. In the case of the other carbon signals there were only negligible changes of the chemical shifts observed.

The ^{13}NMRs of the osmium complexes were very similar for the ruthenium analogues. The signals of the carbonyl C4 and of C3 are shifted upfield (10 ppm and 2 ppm, respectively), whereas the signals of the C5 and C6 are shifted to lower fields (7 ppm and 8 ppm, respectively). The impact of the organometallic coordination on the chemical shift of the other carbons was negligible.

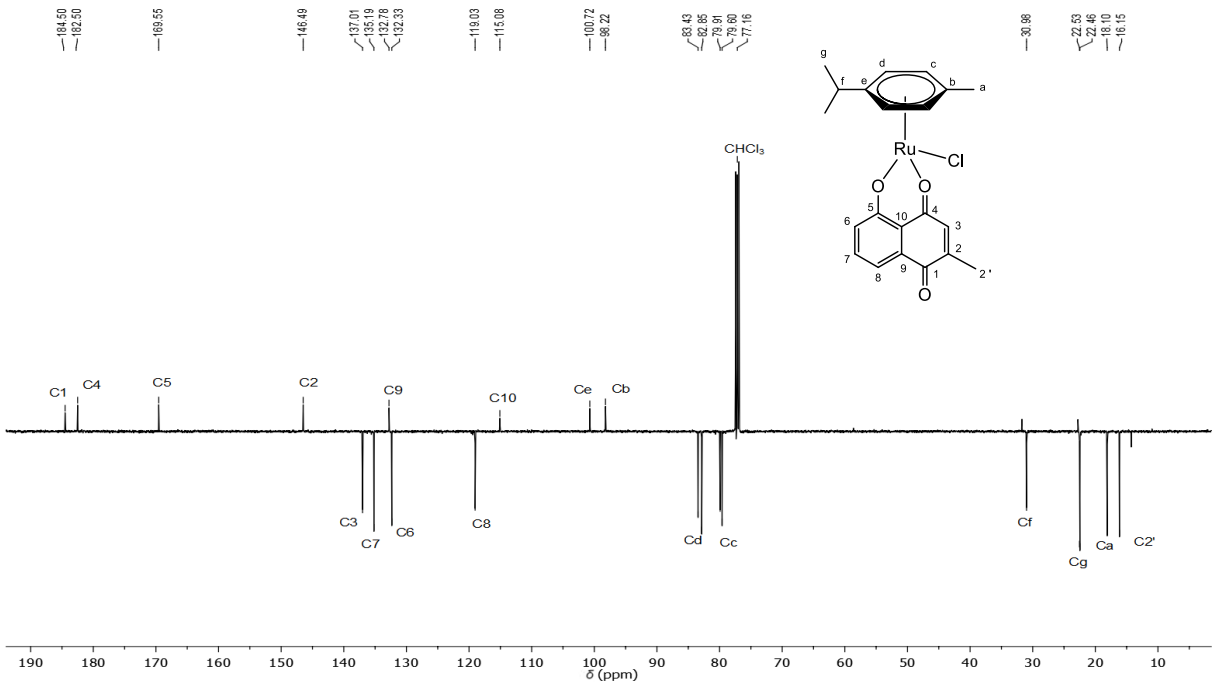

Figure 17: ^{13}C-NMR of **1a**

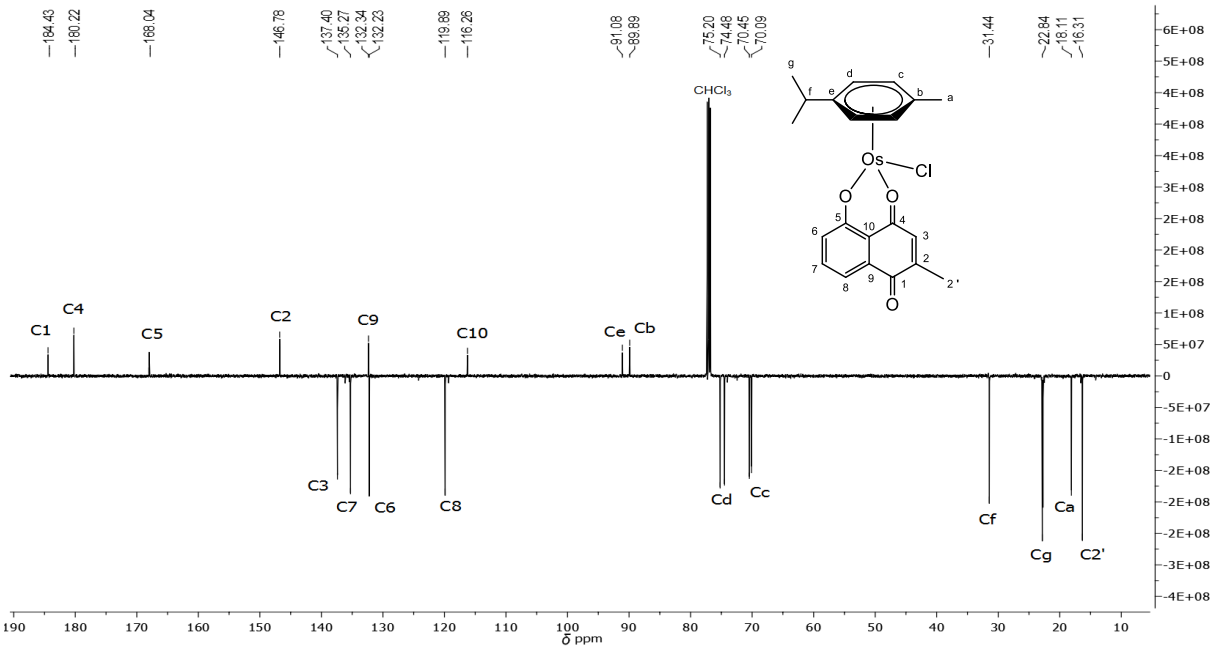

Figure 18: ^{13}C-NMR of **2a**

2D-NMR

All detected signals were assigned via ^{1}H-^{1}H-COSY, ^{1}H-^{13}C-HSQC and ^{1}H-^{13}C-.HMBC. The 2D spectra of compound **1a**are exemplary illustrated below.

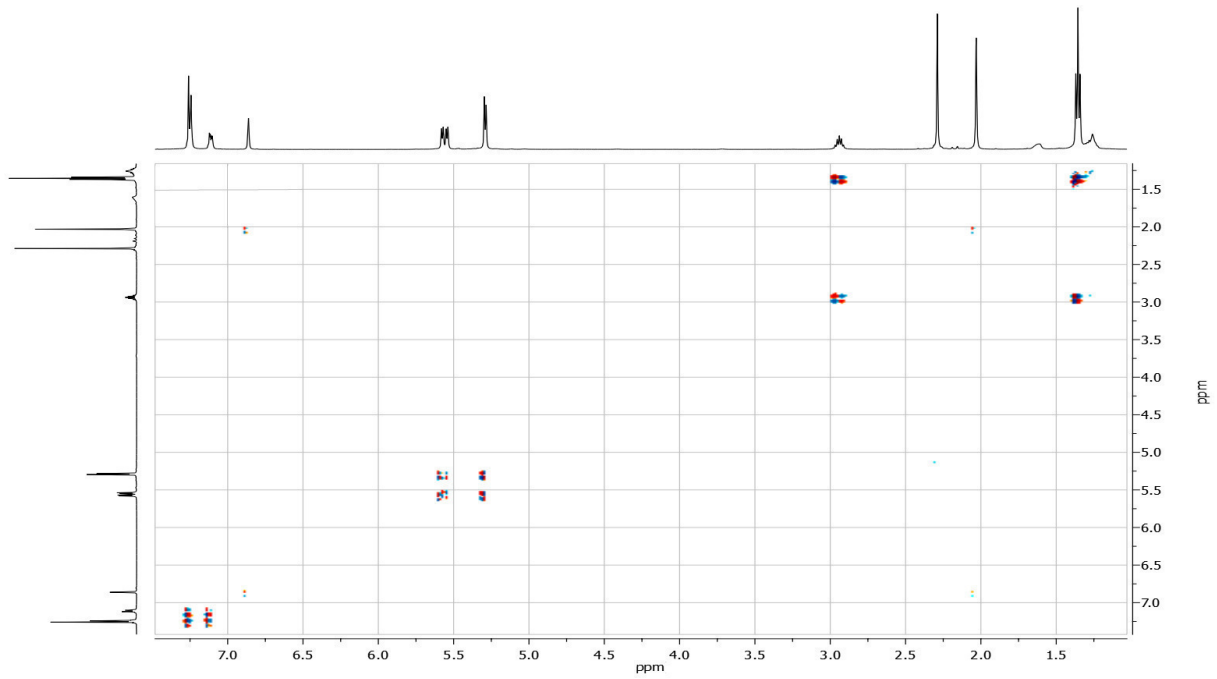

Figure 19: ^{1}H-^{1}H-COSY of **1a**

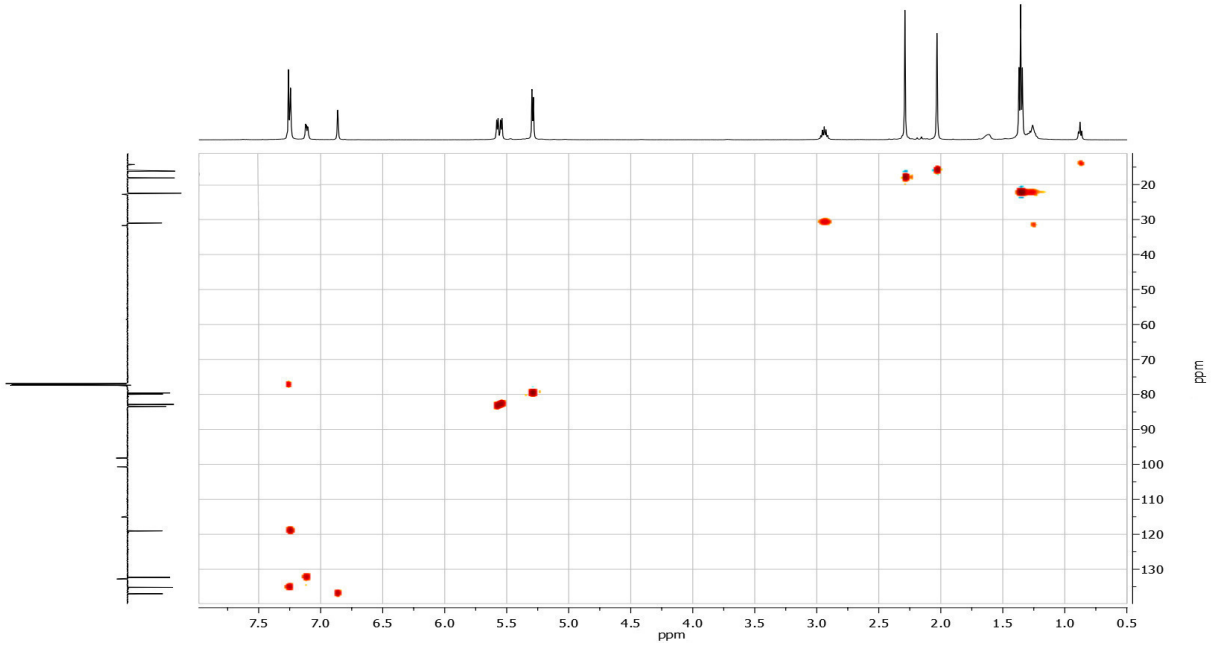

Figure 20: ^{1}H-^{13}C-HSQC of **1a**

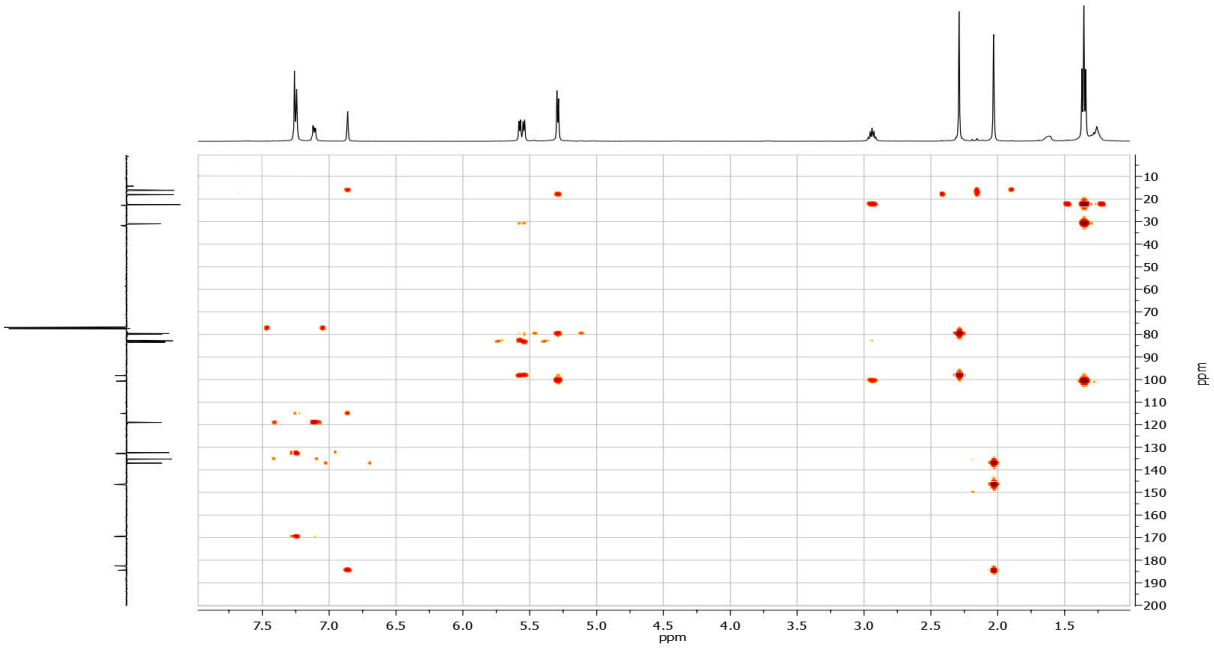

Figure 21: ^{1}H-^{13}C-.HMBC of **1a**

HR-MS

High resolution spectrometry was applied to additionally verify the formation of the synthesized complexes. The compounds were dissolved in acetonitrile/methanol (1:1) with 1% H_2O and the measurements were recorded in positive mode employing direct infusion electrospray ionization and a quadrupole time-of-flight detector. In all cases only the $[M\text{-}Cl]^+$ fragment of the respective complexes was observed (table 1)(Fig. 22). The experimentally found isotope pattern of the peaks is in accordance with the calculated isotope distribution (Fig. 22).

Table 1: Found and calculated values of the synthesized complexes

Complex ion	**m/z**	
$[M\text{-}Cl]^+$	found	calculated
1a	423.0539	423.0534
1b	409.0378	409.0377
1c	500.0804	500.0799
2a	513.1104	513.1096
2b	499.0947	499.0940

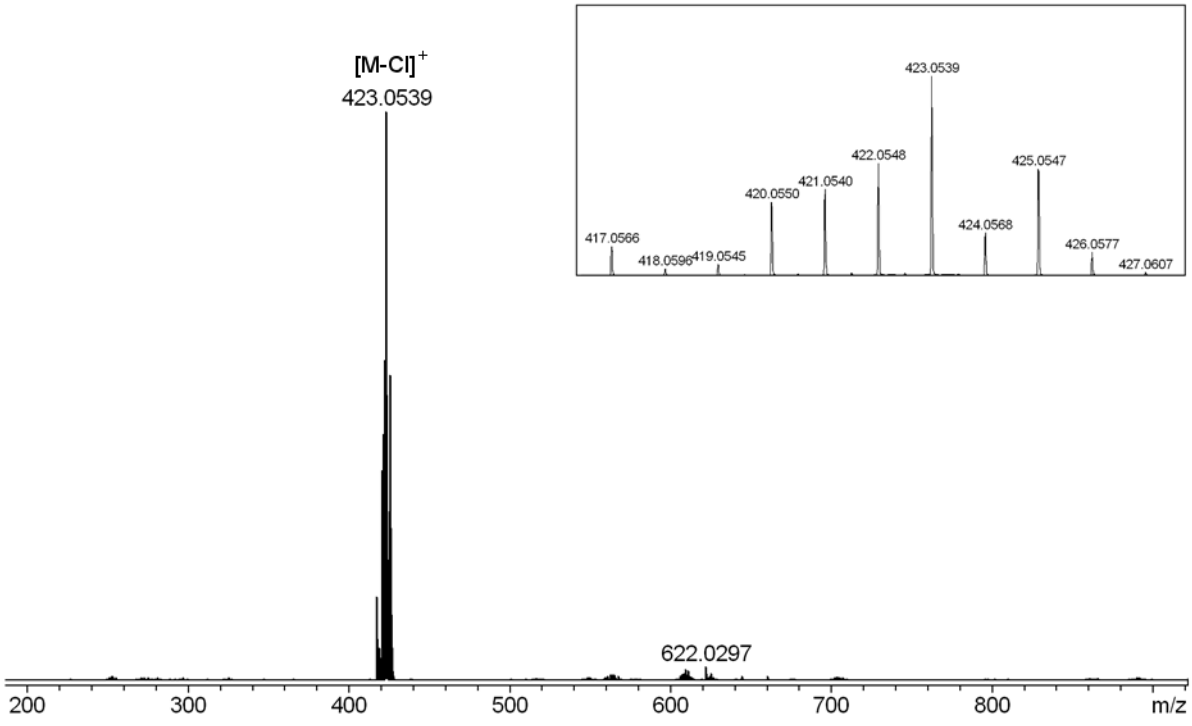

Figure 22: High resolution mass spectrum of compound **1a** with the isotopic distribution pattern

X-ray diffraction analysis

Single crystals of **1a,b** and **2a,b** were obtained via slow diffusion method from dichloromethane/*n*-hexane or benzene/*n*-hexane solutions. All four complexes adopted the so-called “piano-stool” configuration, with the η^6-p-cymene arene being the seat, while the 5-hydroxy-[1,4]-naphthoquinone and the chlorido ligands representing the legs.

The Ru^{II}/Os^{II} complexes of plumbagin, **1a** and **2a,** both crystallize in the monoclinic Cc space group, whereas the respective juglone complexes **1b** and **2b** are representatives of the orthorhombic Pbca space group. In terms of bond lengths and angles the Ru^{II} and the Os^{II} complexes are almost identical, whereas between juglone and plumbagin compounds only small differences were observed.

The six membered ring coordination ring is non-planar in all four compounds, which can be seen from the respective torsion angles M1-O3-C5-C10 [(°) **1a**: 2.9(7), **2a**: 1.6(13), **1b**: 16.8(4), **2b**: 16.0(4)] and M1-O2-C4-C10 [(°) **1a**: 7.45(5), **2a**: -6.9(8), **1b**: -6.8(5), **2b**: -7.6(4)], The carbonyl bond O2-C4 [(Å) **1a**: 1.263(4), **2a**: 1.272(6), **1b**: 1.263(4), **2b**:1.268(3)] is slightly shorter than O3-C5 [(Å) **1a**: 1.296(5), **2a**: 1.304(8), **1b**: 1.291(4), **2b**: 1.291(3)]. Furthermore the bond of O2-C4 in **1a** and **2a** are elongated compared to the free ligand [(Å) **plu**: 1.229(7)][75], whereby there is no change of the respective bond observed in the coordinated juglone [(Å) **jug**: 1.26(2)][76]. In contrary O3-C5 is shortened compared to the uncoordinated species [(Å) **plu**: 1.257(9), **jug**: 1.33(2)]. In all compounds the complexation leads to slightly shortened carbon bonds of C4-C10 [(Å)**1a**: 1.430(5), **2a**: 1.422(7), **plu**: 1.460(8), **1b**: 1.438(4), **2b**: 1.433(4), **jug**: 1.51(2)] and C5-C10 [(Å)**1a**: 1.418(7), **2a**: 1.421(13), **plu**: 1.23(9), **1b**: 1.425(4), **2b**: 1.420(4), **jug**: 1.40(2)]. Also the planarity of the two carbon rings is abolished by the electron withdrawal of the metal, displayed by the torsion angle C8-C9-C10-C4 [(°) **1a**: 172.5(3), **2a**: 171.7(5), **1b**: -174.5(3), **2b**: -174.9(2)]. With a distance of over 3.9 Å between the 5-hydroxy-[1,4]-naphthoquinone ligands of the complexes in the unit cell, it can be assumed that there is no interaction through π-stacking, which typical occurs in a distance between 3.3 to 3.8 Å.[77]

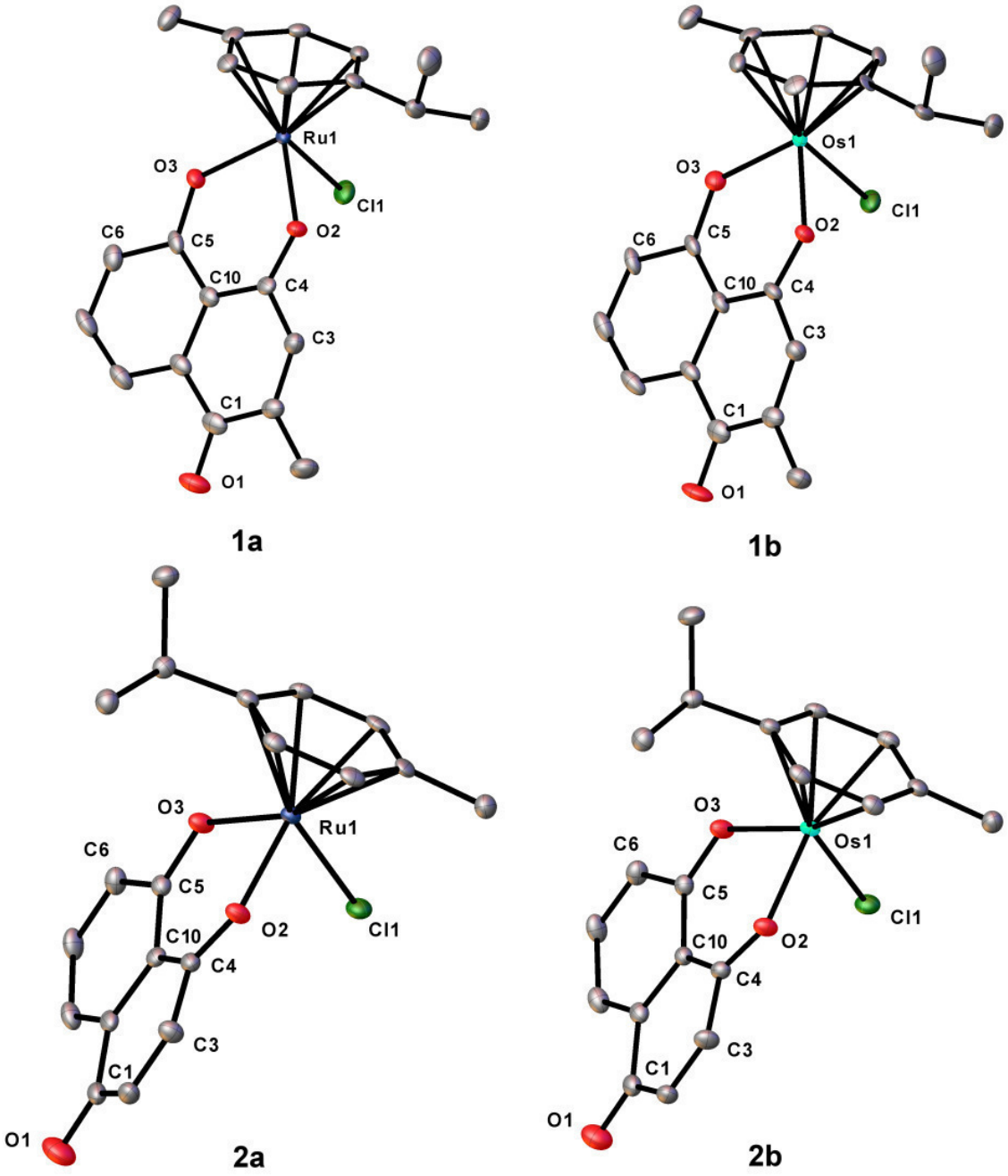

Figure 23: Crystal structures for the compounds **1a-b** and **2a-b** (the hydrogen atoms were omitted for clarity)

Table 2: Bond lengths, bond angles and torsion angles of **1a-b** and **2a-b**

		1a	**2a**	**1b**	**2b**
M-Cl1	[Å]	2.4051(9)	2.4045(13)	2.4154(8)	2.4137(6)
M-O2	[Å]	2.060(2)	2.070(4)	2.084(2)	2.0901(18)
M-O3	[Å]	2.058(2)	2.059(4)	2.052(2)	2.0598(19)
O1-C1	[Å]	1.234(5)	1.237(7)	1.241(4)	1.246(3)
O2- C4	[Å]	1.263(4)	1.272(6)	1.263(4)	1.268(3)
O3- C5	[Å]	1.296(5)	1.304(8)	1.291(4)	1.291(3)
C3-C4	[Å]	1.473(5)	1.471(7)	1.471(4)	1.462(4)
C4-C10	[Å]	1.430(5)	1.422(7)	1.438(4)	1.433(4)
C5-C6	[Å]	1.432(5)	1.435(9)	1.432(4)	1.429(4)
C10-C5	[Å]	1.418(7)	1.421(13)	1.425(4)	1.420(4)
Cl1-M-O2	[°]	83.94(7)	82.86(10)	86.74(6)	85.24(5)
Cl1-M-O3	[°]	85.72(7)	84.54(11)	84.78(7)	83.63(6)
O2-M-O3	[°]	87.07(10)	86.82(14)	85.75(9)	84.96(7)
M-O3-C5	[°]	127.8(3)	128.1(5)	126.7(2)	127.86(17)
M-O2-C4	[°]	128.7(2)	128.6(4)	127.7(2)	128.34(17)
O2-C4-C3	[°]	114.2(3)	113.2(5)	115.3(3)	115.2(2)
O3-C5-C6	[°]	116.0(5)	116.6(9)	115.9(3)	116.0(2)
C8-C9-C10-C4	[°]	172.5(3)	171.7(5)	-174.5(3)	-174.9(2)
M1-O2-C4-C10	[°]	-7.45(5)	-6.9(8)	-6.8(5)	-7.6(4)
M1-O3-C5-C10	[°]	2.9(7)	1.6(13)	16.8(4)	16.0(4)

Table 3: Data collection and refinement parameters for **1a** and **2a**

	1a	**2a**
Empirical formula	$C_{21}H_{21}ClO_3Ru$	$C_{21}H_{21}ClO_3Os$
M [g/mol]	457.91	547.07
T [K]	100.00	100.00
Crystal size [mm]	0.111 × 0.058 × 0.023	0.111 × 0.058 × 0.023
Crystal system	monoclinic	monoclinic
Space group	Cc	Cc
a [Å]	12.6276(6)	12.5841(7)
b [Å]	19.7325(9)	19.7968(10)
c [Å]	7.7139(3)	7.7223(4)
α [°]	90	90
β [°]	106.801(2)	107.1000(17)
γ [°]	90	90
V [Å^3]	1840.05(14)	1838.77(17)
Z	4	4
ρ [g/cm^3]	1.653	1.976
***h* range**	-15/15	-16/16
***k* range**	-24/24	-26/26
***l* range**	-9/9	-10/10
No. reflections	30716	22003
No. Parameters	239	239
R_{int}	0.0406	0.0390
R_{sigma}	0.0229	0.0391
WR_2	0.0421	0.0373
GOF	1.070	1.022

Table 4: Data collection and refinement parameters for **1b** and **2b**

	1b	**2b**
Empirical formula	$C_{20}H_{19}ClO_3Ru$	$C_{20}H_{19}ClO_3Os$
M [g/mol]	443.89	543.05
T [K]	100.00	100.00
Crystal size [mm]	0.1 × 0.1 × 0.08	0.1 × 0.1 × 0.08
Crystal system	orthorhombic	orthorhombic
Space group	Pbca	Pbca
a [Å]	15.8759(4)	15.9048(4)
b [Å]	9.7037(2)	9.7276(2)
c [Å]	21.6680(5)	21.6447(5)
α [°]	90.00	90.00
β [°]	90.00	90.00
γ [°]	90.00	90.00
V [Å^3]	3338.06(13)	3348.77(13)
Z	8	8
ρ [g/cm^3]	1.766	2.114
***h* range**	-19/19	-22/22
***k* range**	-11/11	-13/13
***l* range**	-26/26	-30/30
No. reflections	50720	40027
No. Parameters	229	229
R_{int}	0.0640	0.0330
R_{sigma}	0.0200	0.0191
WR_2	0.0847	0.0449
GOF	1.175	1.091

Stability investigations by UV/Vis spectroscopy

The stability of the ruthenium and osmium compounds **1a–c** and **2a,b** was studied in 1% v/v DMF/PBS *via* UV/Vis spectroscopy. The spectra were measured in DMF, due to the limited stability of the complexes in DMSO. UV/Vis spectra of the complexes in solution were recorded at 25 °C in one hour intervals over 24 hours. An isobestic point with a peak maximum at 336 nm was observed for all five compounds, shifting to lower absorbance with time, reaching half of its height after approximately 4 hours. Both the ruthenium and osmium complexes showed great changes in the spectra, leading to the assumption that hydrolysis is taking place and the compounds are not stable in aqueous solution.

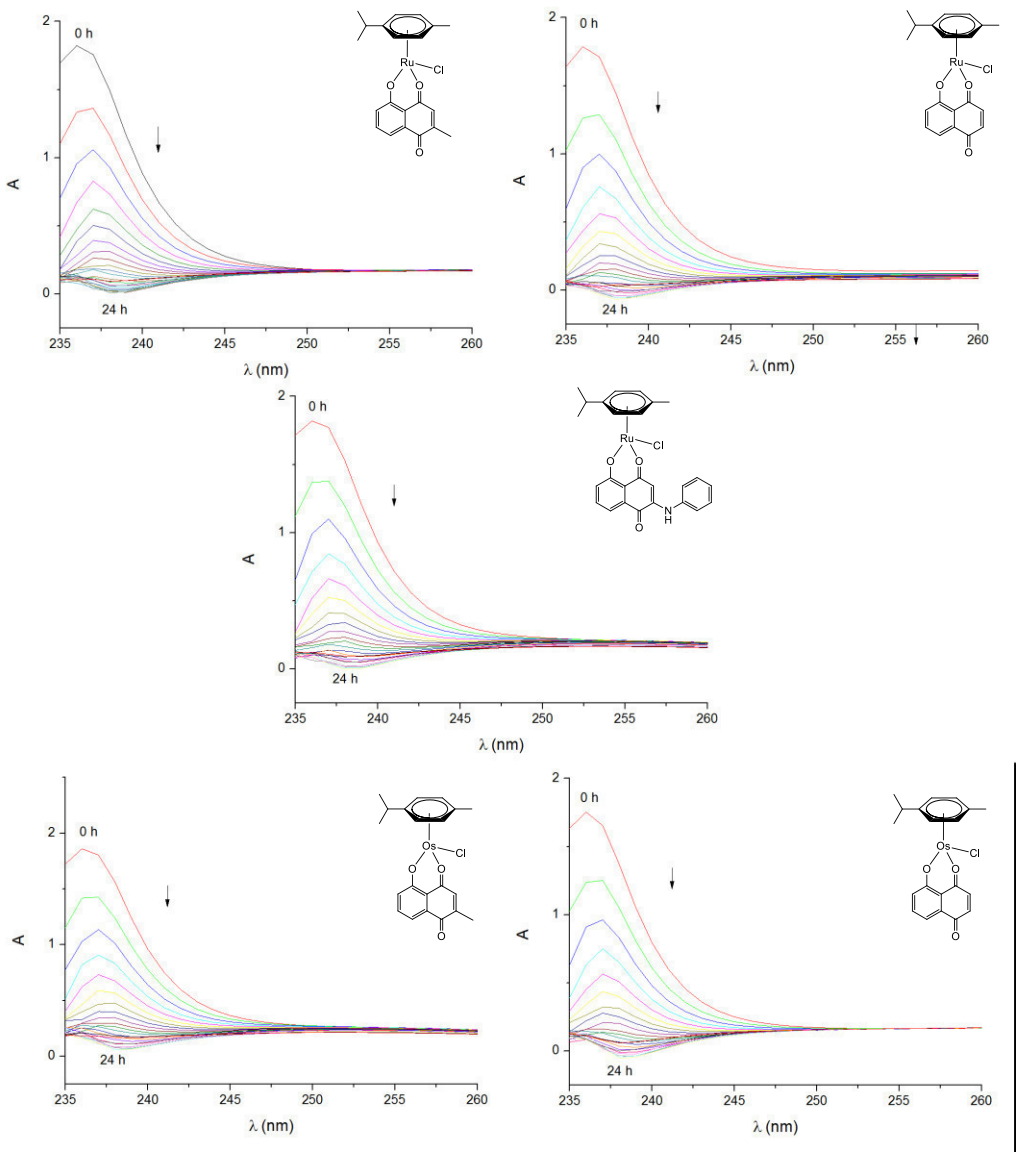

Figure 24: UV/Vis spectra of the ruthenium and osmium complexes.

Cyclovoltammetric investigations of the complexes

The electrochemical behavior of the complexes and their respective ligands was investigated via cyclic voltammetry employing a three-electrode cell with a glassy carbon working electrode, a platinum auxiliary electrode and an $Ag|Ag^{+}$ reference electrode containing. The potentials were measured in DMF containing 0.1 M [n-Bu4N][BF4], using ferrocene as internal standard.

The voltammograms of plumbagin and juglone exhibit two successive reversible one-electron reduction processes typical for quinones in aprotic media.[78] The first peak is associated with the reduction of the quinone into a radical anion or semiquinone ($Q + e^{-} \leftrightarrow Q^{\bullet -}$), while the second peak is connected to reduction of the semiquinone into a dianion species ($Q^{\bullet -} + e^{-} \leftrightarrow Q^{2-}$).

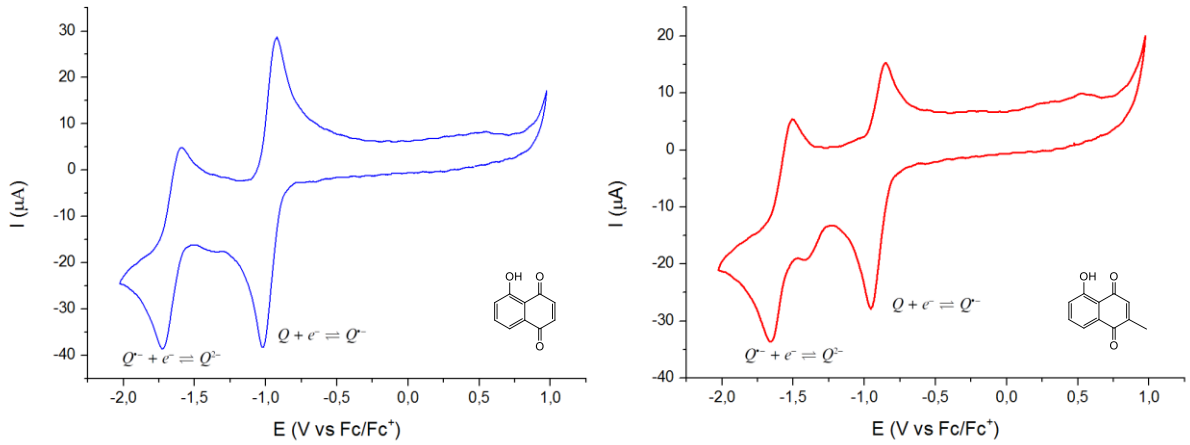

Figure 25: Voltammograms of plumbagin and juglone

In the voltammograms of the respective ruthenium and osmium complexes of juglone and plumbagin the first reversible one-electron reduction processes is also observed in the similar potential range of -0.87 V to -0.99 V (Tab. 5), while the second reversible electron uptake around – 1.6 V does not appear. The complexes also show an irreversible oxidation peak in the range of 0.55 V to 0.82 V, presumably the oxidation from Ru^{II}/Os^{II} to Ru^{III}/Os^{III}. There appears to be another small reversible/irreversible peak around -0.5 V, especially noticeable in compound **2b**.

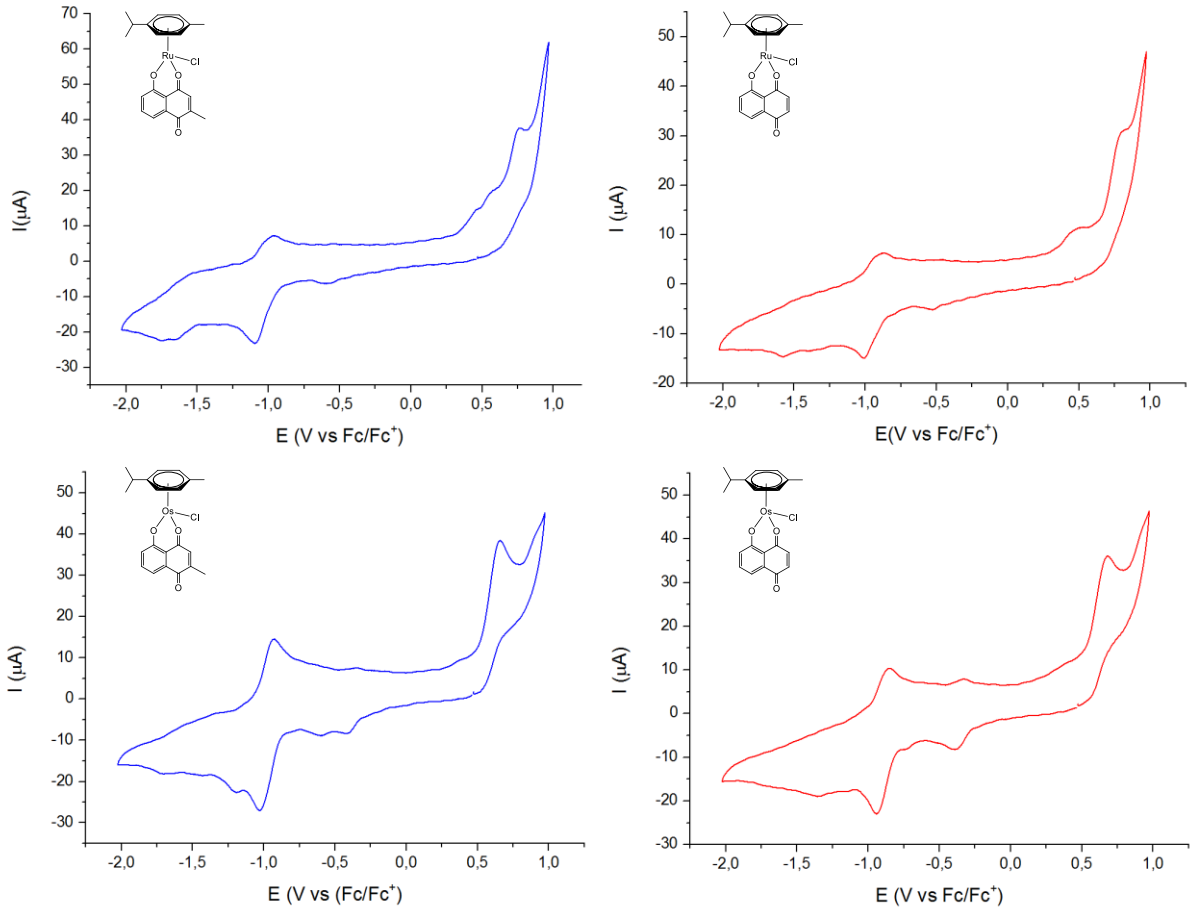

Figure 26: Voltammograms of compounds **1a-b** and **2a-b**

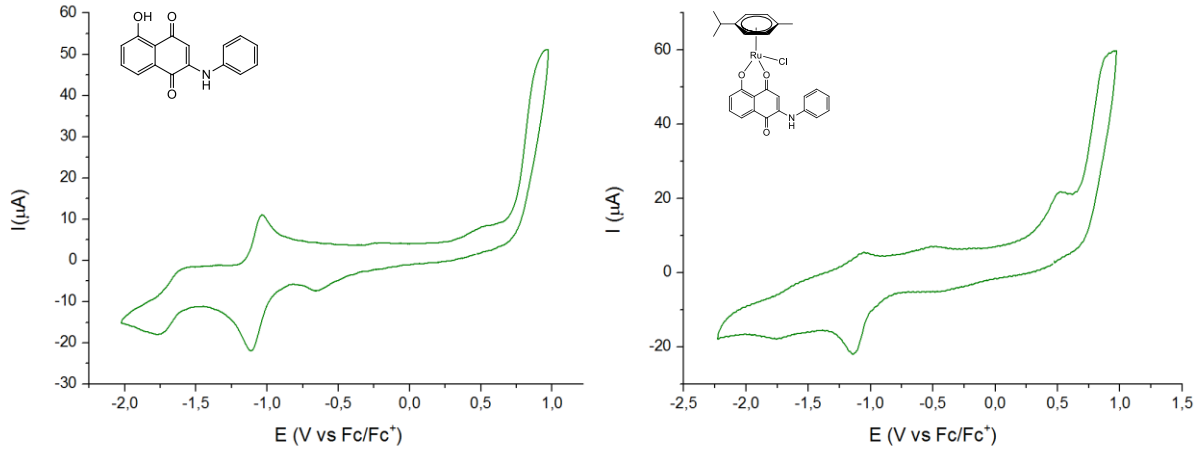

Figure 27: Voltammograms of the ligand **L1** and the compound **1c**

The ligand **L1** also exhibits the two successive reversible one-electron reduction processes, although the second peak is barely noticeable. The measured potential values for **L1** are slightly lower (around 0.1 V to 0.2 V) compared to juglone and plumbagin, which also is observed in the respective complex **1c**.

Table 5: Measured potential values of the reversible and irreversible Peaks against the internal standard ferrocen

E (V vs Fc/ Fc^+)		
Compound	**$E_{1/2}$**	**irrev. Peak**
Plu	-0.94/ -1.64	-
Jug	-0.87/ -1.54	-
L1	-1.04/ -1.67	-
1a	-0.99	0.79
1b	-0.92	0.82
1c	-1.08	0.55
2a	-0.95	0.68
2b	-0.87	0.71

Other ligands and complexes

Additionally, attempts to exchange the chloride leaving group by imidazole and 1-methylimidazole were undertaken. Compound **1a** was employed as precursor and $AgNO_3$ was used for the removal of the chlorido ligand, followed by the addition of the respective N-donor ligand. The counterion was changed to PF_6^- for improved crystallization of the product.

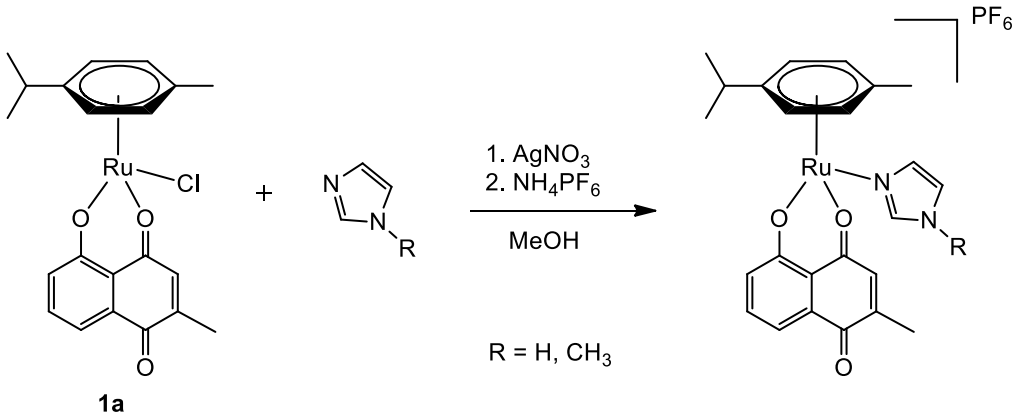

During the reaction the plumbagin ligand was partially cleaved off, directly correlated to the amount of used $AgNO_3$, leading to the formation of two ruthenium p-cymene side products. Presumably the formed intermediate aqua complex was not stable enough and led to the partially decomposition of the complex. Unfortunately it was not possible to completely separate the side products from the product. Nevertheless an X-ray structure of the imidazole complex could be obtained.

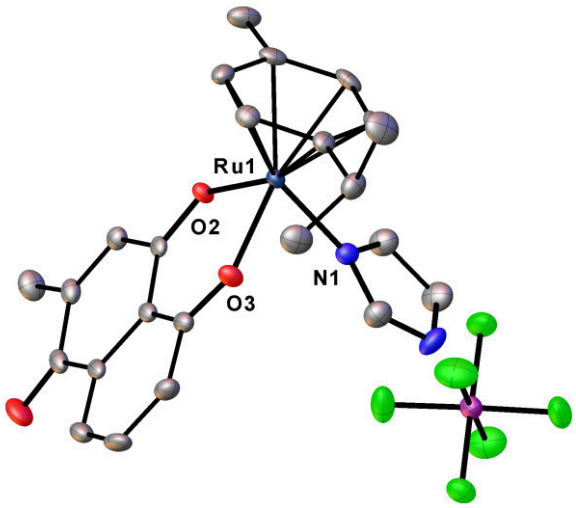

Figure 28: X-ray structure of the imidazole complex (the hydrogen atoms were omitted for clarity)

Furthermore half-sandwich complexes of rhodium(III) and (η^5-1,2,3,4,5-pentamethylcyclopentadienyl) employing 5-hydroxy-[1,4]-naphthoquinones as ligand scaffolds were synthesized. The procedure was similar to the ruthenium compounds, except that the solution was just stirred at room temperature for one hour without any microwave assistance.

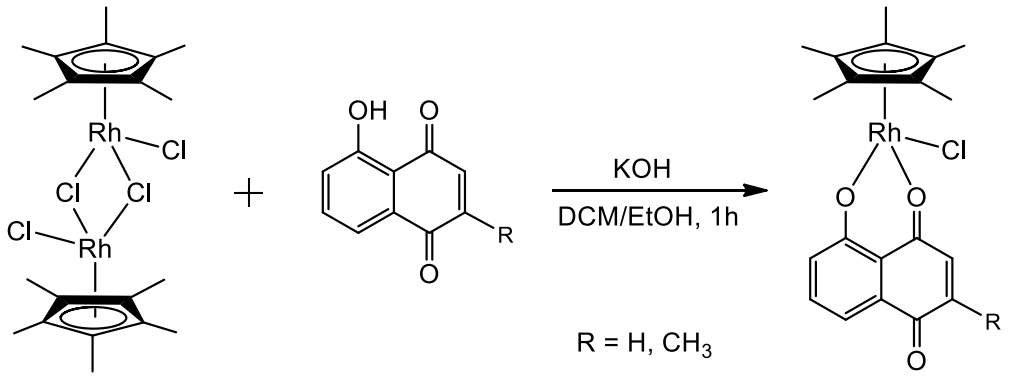

Although it was possible to obtain the crude rhodium products, the complexes were not stable in solution. Decomposition of the complex in $CHCl_3$ was already observed shortly after dissolving and also in other solvents such as MeOH or DMSO the complexes decompose rapidly. Therefore no further characterization of the rhodium compounds was undertaken.

5-Hydroxy-[1,4]-naphthoquinone derivatives of the CDC25 phosphatase inhibitors Cpd 5 and NSC 95397 were successfully synthesized by the addition of 2-mercaptoethanol to juglone or plumbagin.

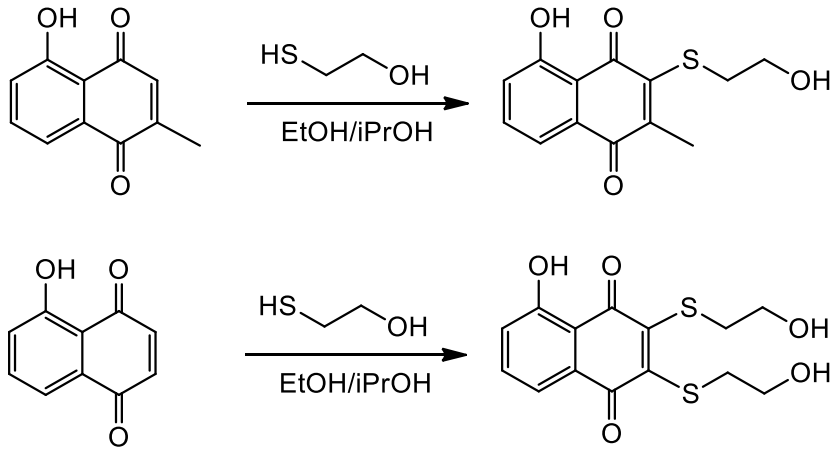

Unfortunately it was not possible to afford the desired complex employing this kind of ligand scaffold.

3 Experimental Part

3.1 Methods and Materials

Elemental analysis

Elemental analyses were performed with a PerkinElmer *2400 Series II CHNS/O Elemental Analyzer* for CHN analyses, and a Eurovector *EA3000 Elemental Analyzer* for CHNS analyses at the Microanalytical Laboratory of the University of Vienna.

Melting points

Melting points were measured with a Büchi *Melting Point M-560*.

X-ray structures

Crystal structures were measured by x-ray diffraction on a Bruker *D8 Venture* system with a multilayer monochromator and a Mo K/a INCOATEC microfocus sealed tube (λ = 0.71073 Å) spectrometer at 100 K.

HR-MS

High resolution mass spectra were recorded on a Bruker *Maxis UHR qTOF Mass Spectrometer* by direct infusion at the Core Facility for Mass Spectrometry (Faculty of Chemistry, University of Vienna).

UV/Vis spectroscopy

UV/Vis spectra were recorded on a PerkinElmer *Lambda 35* UV/Vis spectrometer at 25 C.

NMR

NMR spectra were recorded at 25 °C using a *Bruker FT-NMR spectrometer Avance III^{TM} 500* MHz in chloroform ($CDCl_3$) or deuterated dimethyl sulfoxide (DMSO-d_6). Gradient-enhanced mode was used for the measurement of the 2D NMR spectra.

Solubility

The determination of the solubility was executed in a phosphate buffered saline solution (pH 7.4) containing 1% DMF. The compound was dissolved in DMF and then diluted with PBS to a final concentration of 1% DMF/PBS. The maximum solubility refers to the highest concentration of the analyte where no precipitation could be noticed.

Microwave assisted reactions

For the microwave assisted reactions, a CEM Microwave System Discover SP with Explorer 12 Hybrid autosampler, and the reactions were performed in 10 mL or 35 mL microwave vials with medium stirring and 50 W. All microwaved assisted reactions were performed under Ar atmosphere.

Cyclic voltammetry

Cyclic voltammetry was performed with a three-electrode cell using a glassy carbon working electrode (2.0 mm/ 3.0 mm-diameter), a platinum auxiliary electrode and an $Ag|Ag^+$ reference electrode containing 0.1 M $AgNO_3$ and 10 mM [n-Bu4N][BF4] in DMF. Measurements were executed at room temperature using an EG & G PARC 273A potentiostat/galvanostat at a scan rate of 100 mVs^{-1}. Deaeration of solutions was practiced by passing a stream of argon through the solution for several minutes. The potentials were measured in DMF containing 0.1 M [n-Bu4N][BF4], using ferrocene as internal standard.

Solvents

All solvents were purchased from commercial sources and used without further purification.

Chemicals

Juglone (97%, Acros), plumbagin (98%, Aldrich), aniline (>99.5 %, Aldrich), α-terpinene (90+%, Alfa), cerium(III) chloride heptahydrate (99%, Alfa), ruthenium(III) chloride hydrate (Johnson Matthey) were purchased from commercial suppliers and used without further purification. The precursor $[Os(p\text{-cymene})Cl_2]_2$ was prepared as described in literature.[79]

3.2 Synthesis of the ligand

Synthesis of 5-hydroxy-2-(phenylamino)-[1,4]-naphthoquinone (L1)

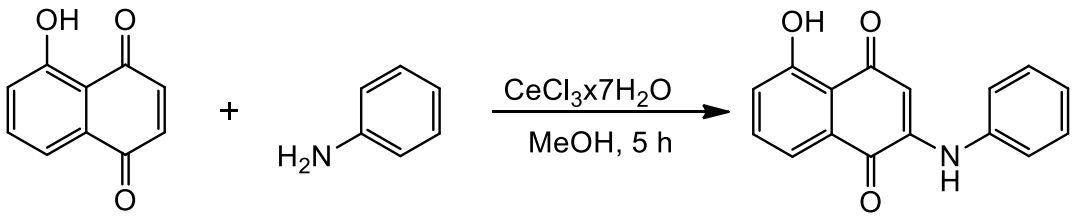

$C_{10}H_6O_3$
174.15 g/mol

C_6H_7N
93.13 g/mol

$C_{16}H_{11}NO_3$
265.26 g/mol

A solution of 5-hydroxy-[1,4]-naphthoquinone (200 mg, 1.15 mmol, 1 eq) and $CeCl_3x7H_2O$ (1 mg, 0.0027 mmol, 0.002 eq) in 12 mL MeOH was sonificated at room temperature for 30 min. Aniline (0.1 mL, 1.15 mmol, 1 eq) was added and the solution was reacted for further 5 h, while keeping the reaction mixture at room temperature. The formed red precipitate was separated by filtration, washed with cold MeOH and dried *in vacuo*. The product was obtained as a red solid.

Yield: 168 mg (55 %)

NMR

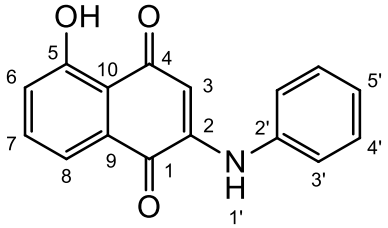

^{1}H NMR (500.10 MHz, DMSO-d^6) δ = 11.54 (s, 1H, OH), 9.28 (s, 1H, H1'), 7.76 – 7.70 (m, 1H, H7), 7.46 (s, 1H, H8), 7.44 (d, ^{3}J = 7.5, 2H, H4'), 7.38 (d, ^{3}J = 7.5 Hz, 2H, H3'), 7.24 - 7.21 (m, 2H, H6, H5'), 6.03 (s, 1H, H3).

^{13}C NMR (126.75 MHz, DMSO-d^6) δ = 185.6 (C1), 181.9 (C4), 160.5 (C5), 146.3 (C2), 138.0 (C2'), 137.6 (C7), 133.0 (C9), 129.4 (C4'), 125.5 (C5'), 123.9 (C3'), 122.3 (C6), 117.7 (C8), 114.4 (C10), 102.2 (C3).

Solubility: <0.01 mg/mL (1% v/v DMF/PBS)

3.3 Synthesis of the complexes

Bis[dichlorido(η^6-*p*-cymene)ruthenium(II)] (1)

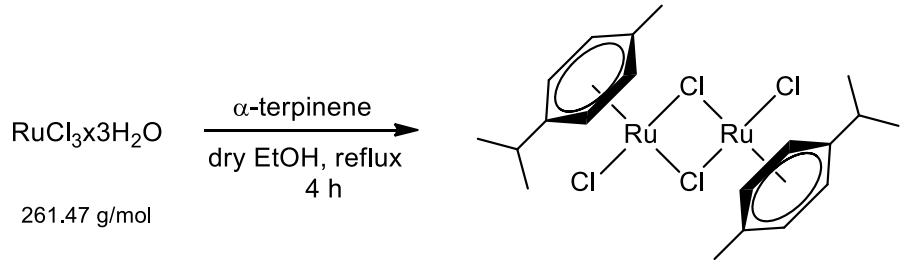

$RuCl_3 \cdot 3H_2O$ (1.00 g, 3.8 mmol, 1 eq) was dissolved in dry EtOH (3.8 mL) and α-terpinene (6.25 mL, 38.4 mmol, 10 eq) was added. The reaction mixture was refluxed under an Ar atmosphere for 4 h. The reaction mixture was allowed to cool to room temperature and reduced to half its volume. The product was precipitated by addition of diethyl ether and was isolated by filtration, washed with diethyl ether and dried *in vacuo.* The precursor complex **1** was obtained as red crystals in excellent yield.

Yield: 1.12 g (96 %)

NMR

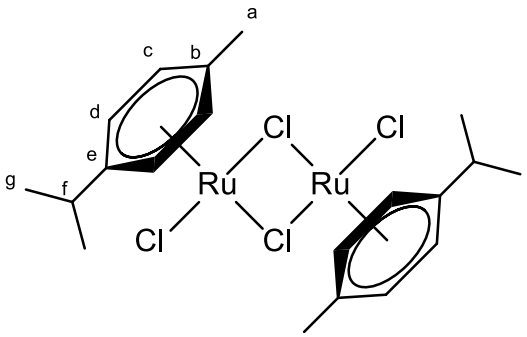

^{1}H NMR (500.10 MHz, $CDCl_3$) δ = 5.47 (d, ^{3}J = 6.0 Hz, 4H, Hd), 5.34 (d, ^{3}J = 6.0 Hz, 4H, Hc), 2.97 – 2.88 (m, 2H, Hf), 2.16 (s, 6H, Ha), 1.28 (d, ^{3}J = 7.0 Hz, 12H, Hg).

Chlorido[2-methyl-5-oxo-*κO*-[1,4]-naphthoquinonato-*κO*](η^6-*p*-cymene)ruthenium(II) (1a)

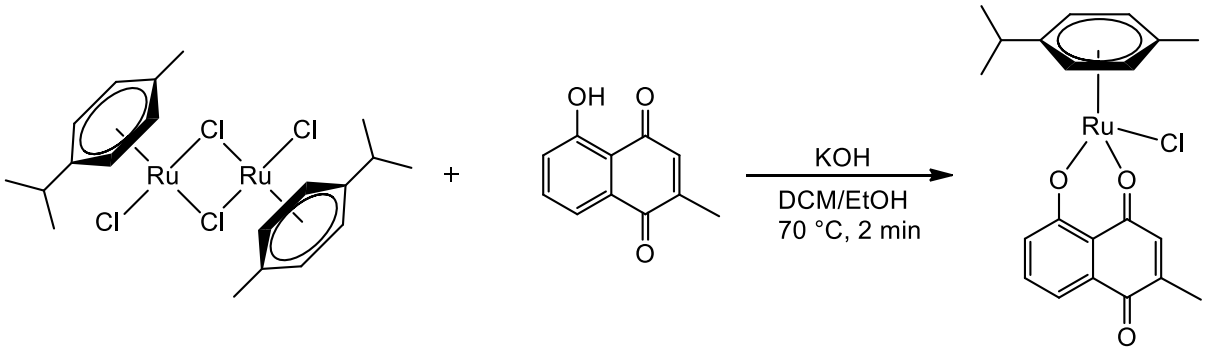

$C_{20}H_{28}Cl_4Ru_2$
612.39 g/mol

$C_{11}H_8O_3$
188.18 g/mol

$C_{21}H_{21}ClO_3Ru$
457.91 g/mol

[Ru(*p*-cymene)Cl_2]$_2$ (95 mg, 0.31 mmol, 0.9 eq) and plumbagin (65 mg, 0.35 mmol, 1 eq) were dissolved with DCM (6.4 mL) and EtOH (96%, 0.9 mL) in a microwave vial. A solution of KOH (23 mg, 0.41 mmol, 1.2 eq) in EtOH (96%, 2.3 mL) was added and irradiated for 2 min at 70 °C (microwave induced, 50 W). The solution was evaporated to dryness and the residue was taken up in DCM and filtered. An excess of *n*-hexane was added, followed by slow evaporation of DCM. The formed crystals were separated by filtration, washed with *n*-hexane and dried *in vacuo*. The compound **1a** was obtained as a black solid.

Yield: 135 mg, 95%

HRMS: $[M-Cl]^+$ 423.0539 (found)

423.0534 (calculated)

Melting point: 118 - 122°C

Solubility: 0.42 mg/mL (1% v/v DMF/PBS)

Elemental analysis

$C_{21}H_{21}ClO_3Ru$	C[%]	H[%]	O[%]	N[%]
calculated	55.08	4.62	10.48	0.00
found	54.87	4.95	10.31	<0.05
Δ	0.21	0.33	0.17	0.00

NMR

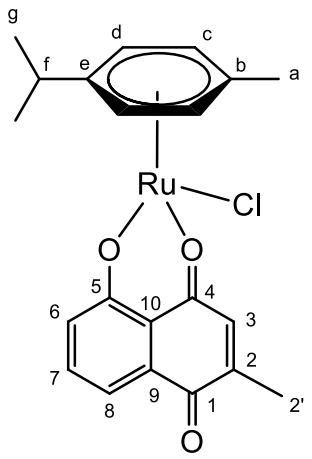

^{1}H NMR (500.10 MHz, $CDCl_3$) δ = 7.25 (1H, H7(under the $CHCl_3$ peak)) 7.24 (s, 1H, H8), 7.11 (dd, ^3J = 6.8 Hz, ^3J = 2.9 Hz, 1H, H6), 6.86 (s, 1H, H3), 5.58 - 5.54 (m, 2H, Hd), 5.29 (d, ^3J = 5.9 Hz, 2H, Hc), 2.98 – 2.90 (m, 1H, Hf), 2.29 (s, 3H, Ha), 2.03 (s, 3H, H2'), 1.36 (t, ^3J = 7.0 Hz, 6H, Hg).

^{13}C NMR (126.75 MHz, $CDCl_3$) δ = 184.5 (C1), 182.5 (C4), 169.6 (C5), 146.5 (C2), 137.0 (C3), 135.2 (C7), 132.8 (C9), 132.3 (C6), 119.0 (C8), 114.7 (C10), 100.7 (Ce), 98.2 (Cb), 83.4 (Cd), 82.8 (Cd), 79.9 (Cc), 79.6 (Cc), 31.0 (Cf), 22.5 (Cg), 18.1 (Ca), 16.2 (C2').

Chlorido[5-oxo-*κO*-[1,4]-naphthoquinonato-*κO*](η^6-*p*-cymene)ruthenium(II) (1b)

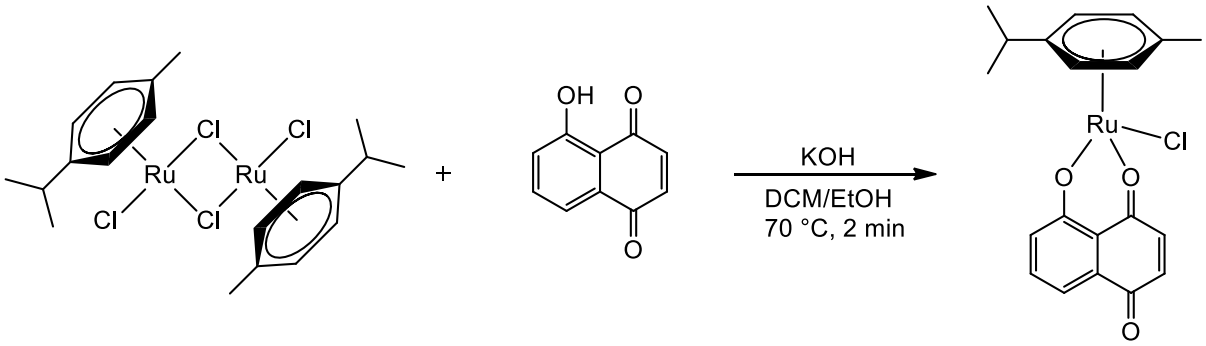

$C_{20}H_{28}Cl_4Ru_2$
612.39 g/mol

$C_{10}H_6O_3$
174.15 g/mol

$C_{20}H_{19}ClO_3Ru$
443.89 g/mol

[Ru(*p*-cymene)Cl_2]$_2$ (40 mg, 0.13 mmol, 0.9 eq) and juglone (25 mg, 0.15 mmol, 1 eq) were dissolved with DCM (2.7 mL) and EtOH (96%, 0.4 mL) in a microwave vial. A solution of KOH (9.8 mg, 0.17 mmol, 1.2 eq) in EtOH (96%, 1.9 mL) was added and irradiated for 2 min at 70 °C (microwave induced, 50 W). The solution was evaporated to dryness and the residue was taken up in DCM and filtered. An excess of n-hexane was added, followed by slow evaporation of DCM. The formed crystals were separated by filtration, washed with n-hexane and dried *in vacuo*. The compound **1b** was obtained as a black solid.

Yield:	56 mg, 97 %
HRMS: $[M-Cl]^+$	409.0378 (found)
	409.0377 (calculated)
Melting point:	161 - 164 °C
Solubility:	0.25 mg/mL (1% v/v DMF/PBS)

Elemental analysis

$C_{20}H_{19}ClO_3Ru$	C[%]	H[%]	O[%]	N[%]
calculated	54.12	4.31	10.81	0.00
found	53.94	4.21	10.59	<0.05
Δ	0.18	0.10	0.22	0.00

i

NMR

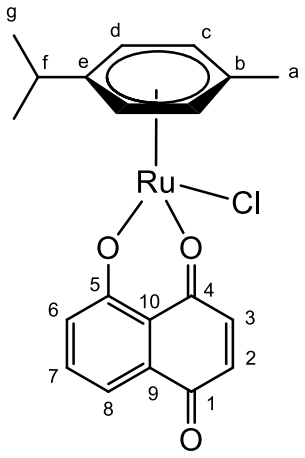

^{1}H-NMR

^{1}H NMR (500.10 MHz, $CDCl_3$) δ = 7.31 – 7.27 (m, 1H, H7), 7.23 (dd, ^{3}J = 6.9 Hz, ^{4}J = 1.1 Hz, 1H, H8), 7.14 (dd, ^{3}J = 8.7 Hz, ^{4}J = 1.1 Hz, 1H, H6), 7.00 (d, ^{3}J = 10.1 Hz, 1H, H2), 6.69 (d, ^{3}J = 10.1 Hz, 1H, H3), 5.60 – 5.56 (m, 2H, Hd), 5.31 (d, ^{3}J = 6.1 Hz, 2H, Hc), 2.98 – 2.90 (m, 1H, Hf), 2.29 (s, 3H, Ha), 1.36 (t, ^{3}J = 7.1 Hz, 6H, Hg).

^{13}C-NMR

^{13}C NMR (126.75 MHz, CDCl3) δ = 184.2 (C1), 182.0 (C4), 170.2 (C5), 140.4 (C2), 136.7 (C3), 135.5 (C7), 132.7 (C9), 132.5 (C6), 119.1 (C8), 115.2 (C10), 100.9 (Ce), 98.4 (Cb), 83.5 (Cd), 82.9 (Cd), 80.1 (Cc), 79.7 (Cc), 31.0 (Cf), 22.5 (Cg), 18.1 (Ca).

Chlorido[5-oxo-*κO*-2-(phenylamino)-[1,4]-naphthoquinonato-*κO*](η^6-*p*-cymene)ruthenium(II) (1c)

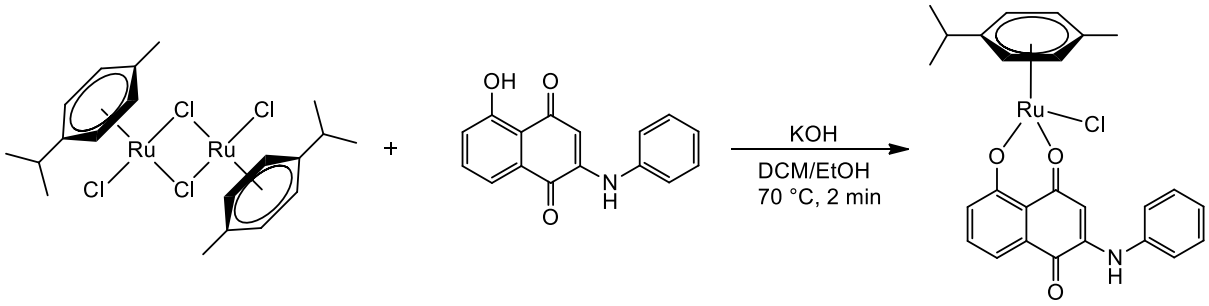

$C_{20}H_{28}Cl_4Ru_2$
612.39 g/mol

$C_{16}H_{11}NO_3$
265.26 g/mol

$C_{26}H_{24}ClNO_3Ru$
536.00 g/mol

[Ru(*p*-cymene)Cl_2]$_2$ (50 mg, 0.16 mmol, 0.9 eq) and **L1** (48 mg, 0.18 mmol, 1 eq) were dissolved with DCM (5.0 mL) and EtOH (96%, 0.8 mL) in a microwave vial. A solution of KOH (17 mg, 0.31 mmol, 1.7 eq) in EtOH (96%, 1.7 mL) was added and irradiated for 2 min at 70 °C (microwave induced, 50 W). The solution was evaporated to dryness and the residue was taken up in DCM and filtered. An excess of *n*-hexane was added, followed by slow evaporation of DCM. The formed crystals were separated by filtration, washed with *n*-hexane and dried *in vacuo*. The compound **1c** was obtained as a black solid.

Yield: 64 mg

HRMS: $[M\text{-}Cl]^+$ 500.0804 (found)

500.0799 (calculated)

Melting point: > 400 °C

Solubility 0.05 mg/mL (1% v/v DMF/PBS)

Elemental analysis

$C_{26}H_{24}ClNO_3Ru \cdot 1.1H_2O$	C[%]	H[%]	O[%]	N[%]
calculated	56.28	4.75	11.82	2.52
found	55.98	4.40	11.63	2.60
Δ	0.30	0.35	0.19	0.08

NMR

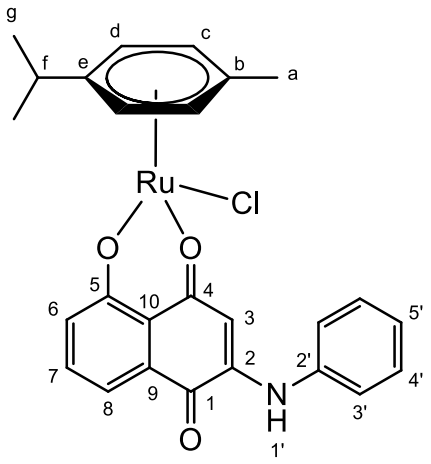

^{1}H-NMR

^{1}H NMR (500.10 MHz, $CDCl_3$) δ = 7.42 – 7.39 (m, 2H, H4'), 7.30 – 7.27 (m, 1H, H7), 7.25 – 7.23 (m, 1H, H3') 7.23 – 7.21 (m, 1H, H5'), 7.20 – 7.18 (m, 1H, H8), 7.04 (d, ^{3}J = 8.7 Hz, 1.0, 1H, H6), 6.37 (s, 1H, H1'), 6.16 (s, 1H, H3), 5.67 – 5.61 (m, 2H, Hd), 5.36 (dd, ^{3}J = 5.6 Hz, ^{3}J = 2.0 Hz, 2H, Hc), 3.00 – 2.92 (m, 1H, Hf), 2.31 (s, 3H, Ha), 1.41 (dd, ^{3}J = 9.5 Hz, ^{3}J = 7.0 Hz, 6H, Hg).

^{13}C-NMR

^{13}C NMR (126.75 MHz, $CDCl_3$) δ = 182.7 (C1), 175.8 (C4), 171.6 (C5), 146.7 (C2), 137.7 (C2'), 136.6 (C7), 133.2 (C9), 129.7 (C4'), 125.7 (C5'), 123.3 (C3'), 122.8 (C6), 118.2 (C8), 114.1 (C10),103.3 (C3), 100.3 (Ce), 98.2 (Cb), 83.8 (Cd), 82.6 (Cd), 79.6 (Cc), 78.9 (Cc), 31.0 (Cf), 22.6 (Cg), 18.1 (Ca).

Chlorido[2-methyl-5-oxo-*κO*-[1,4]-naphthoquinonato-*κO*](η^6-*p*-cymene)osmium(II) (2a)

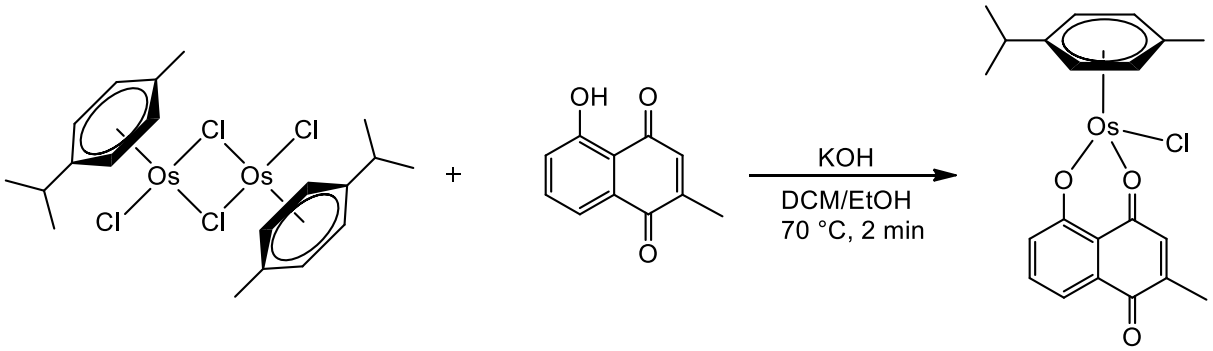

$C_{20}H_{28}Cl_4Os_2$
790.71 g/mol

$C_{11}H_8O_3$
188.18 g/mol

$C_{21}H_{21}ClO_3Os$
547.07 g/mol

[Os(*p*-cymene)Cl_2]$_2$ (170 mg, 0.43 mmol, 0.9 eq) and plumbagin (90 mg, 0.48 mmol, 1 eq) were dissolved with DCM (11.4 mL) and EtOH (96%, 3 mL) in a microwave vial. A solution of KOH (27 mg, 0.48 mmol, 1 eq) in EtOH (96%, 3.2 mL) was added and irradiated for 2 min at 70 °C (microwave induced, 50 W). The solution was evaporated to dryness and the residue was taken up in DCM and filtered. An excess of *n*-hexane was added, followed by slow evaporation of DCM. The formed crystals were separated by filtration, washed with *n*-hexane and dried *in vacuo*. The compound **2a** was obtained as a black solid.

Yield: 132 mg, 57%

HRMS: $[M-Cl]^+$ 513.1104 (found)

513.1097 (calculated)

Melting point: 178 - 180 °C

Solubility: 0.50 mg/mL (1% v/v DMF/PBS)

Elemental analysis

$C_{21}H_{21}ClO_3Os$	C[%]	H[%]	O[%]	N[%]
calculated	46.10	3.87	8.77	0.00
found	46.05	3.92	8.54	<0.05
Δ	0.05	0.05	0.23	0.00

NMR

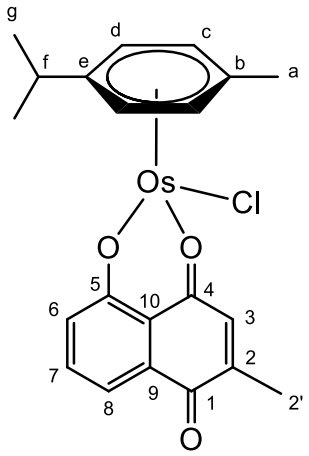

^{1}H NMR (500.10 MHz, $CDCl_3$) δ = 7.35 (dd, ^{3}J = 7.8 Hz, ^{3}J = 7.8 Hz, 1H, H7), 7.28 (d, ^{3}J = 6.9 Hz, 1H, H8), 7.04 (d, ^{3}J = 8.6 Hz, 1H, H6), 6.84 (s, 1H, H3), 5.99 – 5.96 (m, 2H, Hd), 5.75 (s, 2H, Hc), 2.81 - 2.73 (m, 1H, Hf), 2.30 (s, 3H, Ha), 1.98 (s, 3H, H2'), 1.32 (t, ^{3}J = 6.9 Hz, 6H, Hg).

^{13}C NMR (126.75 MHz, $CDCl_3$) δ = 184.4 (C1), 180.2 (C4), 168.0 (C5), 146.8 (C2), 137.4 (C3), 135.3 (C7), 132.3 (C9), 132.2 (C6), 119.9 (C8), 116.3 (C10), 91.1 (Ce), 89.9 (Cb), 75.2 (Cd), 74.5 (Cd), 70.5 (Cc), 70.1 (Cc), 31.4 (Cf), 22.8 (Cg), 18.1 (Ca), 16.3 (C2').

Chlorido[5-oxo-*κO*-[1,4]-naphthoquinonato-*κO*](η^6-*p*-cymene)osmium(II) (2b)

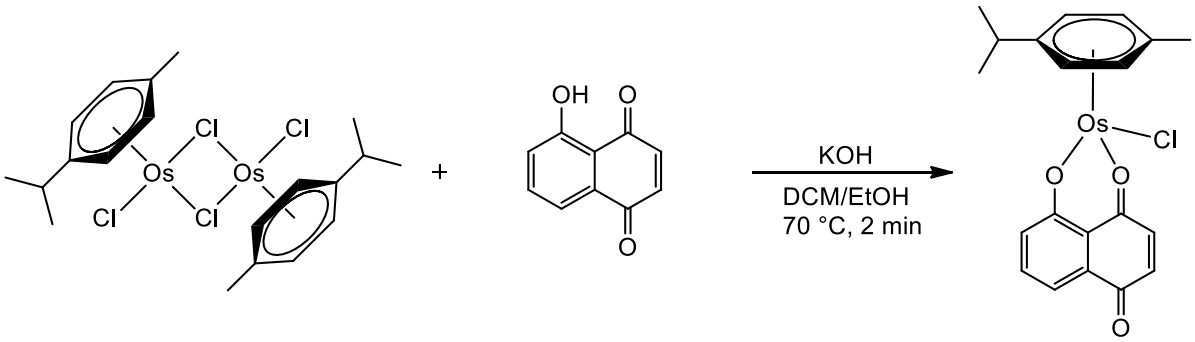

$C_{20}H_{28}Cl_4Os_2$
790.71 g/mol

$C_{10}H_6O_3$
174.15 g/mol

$C_{20}H_{19}ClO_3Os$
533.05 g/mol

$[Os(p\text{-cymene})Cl_2]_2$ (100 mg, 0.25 mmol, 0.9 eq) and juglone (49 mg, 0.28 mmol, 1 eq) were dissolved with DCM (6.7 mL) and EtOH (96%, 1.8 mL) in a microwave vial. A solution of KOH (16 mg, 0.28 mmol, 1 eq) in EtOH (96%, 1.6 mL) was added and irradiated for 2 min at 70 °C (microwave induced, 50 W). The solution was evaporated to dryness and the residue was taken up in DCM and filtered. An excess of *n*-hexane was added, followed by slow evaporation of DCM. The formed crystals were separated by filtration, washed with *n*-hexane and dried *in vacuo*. The compound **2b** was obtained as a black solid.

Yield: 94 mg, 70 %

HRMS: $[M\text{-}Cl]^+$ 499.0947 (found)

499.0940 (calculated)

Melting point: 139 -141 °C

Solubility: 0.42 mg/mL (1% v/v DMF/PBS)

Elemental analysis

$C_{20}H_{19}ClO_3Os \cdot 0.15H_2O$	C[%]	H[%]	O[%]	N[%]
calculated	44.84	3.63	9.41	0.00
found	44.62	3.27	9.17	<0.05
Δ	0.22	0.36	0.24	0.00

NMR

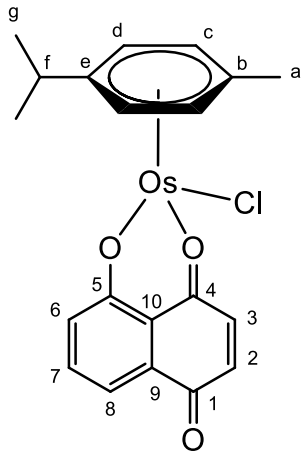

1H-NMR

^{1}H NMR (500.10 MHz, $CDCl_3$) δ = 7.40 (dd, ^{3}J = 8.8 Hz, ^{3}J = 7.0 Hz, 1H, H7), 7.29 – 7.27 (m, 1H, H8), 7.06 (dd, ^{3}J = 8.8 Hz, ^{4}J = 1.0 Hz, 1H, H6), 6.98 (d, ^{3}J = 10.1 Hz, 1H, H2), 6.83 (d, ^{3}J = 10.1 Hz, 1H, H3), 6.01 - 5.98 (m, 2H, Hd), 5.77 (dd, ^{3}J = 5.1 Hz, ^{3}J = 5.1 Hz,2H, Hc), 2.81 – 2.75 (m, 1H, Hf), 2.31 (s, 3H, Ha), 1.32 (t, ^{3}J = 7.0 Hz, 6H, Hg).

13C-NMR

^{13}C NMR (126.75 MHz, $CDCl_3$) δ = 184.3 (C1), 180.1 (C4), 167.5 (C5), 141.1 (C2), 136.8 (C3), 135.8 (C7), 132.7 (C9), 132.1 (C6) 120.12(C8), 116.32(C10), 91.2 (Ce), 89.9 (Cb), 75.4 (Cd), 74.73(Cd), 70.8 (Cc), 70.4 (Cc), 31.6 (Cf), 22.8 (Cg), 18.2 (Ca).

4 Conclusion

Over the duration of this master thesis, a synthetic procedure for the generation of ruthenium (II) and osmium(II) half-sandwich complexes, employing *O*,*O* coordinated 5-hydroxy-[1,4]-naphthoquinone ligands, was developed, leading to five novel metal complexes with moderate to excellent yield (57-97%). Additionally a new 5-hydroxy-[1,4]-naphthoquinone ligand was synthesized. The complexes and the ligand were characterized via 1D/2D $^{1}H/^{13}C$-NMR spectroscopy, high-resolution mass spectrometry and elemental analysis. Furthermore crystal structures of four complexes were obtained by X-ray diffraction analysis and the redox behavior was investigated by cyclic voltammetry. Besides poor solubility in aqueous solution (1% DMF/PBS), all complexes also were prone to decomposition in aqueous medium as indicated by UV/Vis spectroscopy investigations.

Additionally half-sandwich complexes of rhodium(III), employing *O*,*O* coordinated 5-hydroxy-[1,4]-naphthoquinone ligands, were synthesized. However further investigations were not possible due to their vast instability in solution. In the case of the ruthenium complexes it was tried to replace the chloride leaving group by imidazole derivatives, but unfortunately an inseparable product mixture was obtained.

Although an efficient synthetic procedure was developed for *O*,*O* coordinated 5-hydroxy-[1,4]-naphthoquinone half-sandwich complexes, their instability in aqueous medium prevent further biological experiments.

5 References

[1] http://www.who.int/mediacentre/factsheets/fs297/en/

[2] Stewart BW, W. C.; *World cancer report,* **2014**.

[3] Aitken, M.; *Global Oncology Trend Report,* **2016**.

[4] https://www.statistik.at/web_en/statistics/PeopleSociety/health/cancer_incidence/cancer_incidence_overview/index.html

[5] https://www.statistik.at/web_de/statistiken/menschen_und_gesellschaft/gesundheit/krebserkrankungen/krebs_im_ueberblick/index.html

[6] Siddiqui, I.; Sanna, V.; Ahmad, N.; Sechi, M.; Mukhtar, H.; **2015**, *1348*.

[7] Deim, H. D., E., in *Toxikologie. Eine Einführung für Naturwissenschaftler und Mediziner* **1996**, pp. 136, 142-147.

[8] Hanahan, D.; Weinberg, Robert A.; *Cell*, *144*, 646-674.

[9] Witsch, E.; Sela, M.; Yarden, Y.; *Physiology (Bethesda, Md.),* **2010**, *25*, 85-101.

[10] Cheng, N.; Chytil, A.; Shyr, Y.; Joly, A.; Moses, H. L.; *Molecular cancer research : MCR,* **2008**, *6*, 1521-1533.

[11] Levine, A. J.; Momand, J.; Finlay, C. A.; *Nature,* **1991**, *351*, 453-456.

[12] Burkhart, D. L.; Sage, J.; *Nature reviews. Cancer,* **2008**, *8*, 671-682.

[13] Evan, G.; Littlewood, T.; *Science (New York, N.Y.),* **1998**, *281*, 1317-1322.

[14] Blasco, M. A.; *Nature reviews. Genetics,* **2005**, *6*, 611-622.

[15] Folkman, J.; *Seminars in oncology,* **2002**, *29*, 15-18.

[16] Nagy, J. A.; **2010**, *36*, 321-331.

[17] Fang, J.; Nakamura, H.; Maeda, H.; *Advanced drug delivery reviews,* **2011**, *63*, 136-151.

[18] Talmadge, J. E.; Fidler, I. J.; *Cancer research,* **2010**, *70*, 5649-5669.

[19] Negrini, S.; Gorgoulis, V. G.; Halazonetis, T. D.; *Nature reviews. Molecular cell biology,* **2010**, *11*, 220-228.

[20] Qian, B.; Pollard, J. W.; *Cell,* **2010**, *141*, 39-51.

[21] http://www.who.int/cancer/treatment/en/

[22] https://www.cancer.gov/about-cancer/treatment/types

[23] Yardley, D. A.; *International Journal of Breast Cancer,* **2013**, *2013*, 15.

[24a] https://www.cancer.org/treatment/treatments-and-side-effects/treatment-types/chemotherapy/how-chemotherapy-drugs-work.html

[24b] http://chemoth.com/types/antimetabolites

[25] Dabrowiak, J. C., in *Metals in Medicine*, John Wiley & Sons, Ltd, **2009**, pp. 49-72.

[26] Banerjee, S. R.; Pomper, M. G.; *Applied radiation and isotopes : including data, instrumentation and methods for use in agriculture, industry and medicine,* **2013**, *0*, 2-13.

[27] Rosenberg, B.; Vancamp, L.; Trosko, J. E.; Mansour, V. H.; *Nature,* **1969**, *222*, 385.

[28] Ott, I.; Gust, R.; *Pharmazie in unserer Zeit,* **2006**, *35*, 124-133.

[29] Jakupec, M. A.; Galanski, M.; Arion, V. B.; Hartinger, C. G.; Keppler, B. K.; *Dalton transactions (Cambridge, England : 2003),* **2008**, 183-194.

[30] Howell, S. B.; Safaei, R.; Larson, C. A.; Sailor, M. J.; *Molecular pharmacology,* **2010**, *77*, 887-894.

[31] Reedijk, J.; Teuben, J. M., in *Cisplatin*, Verlag Helvetica Chimica Acta, **2006**, pp. 339-362.

[32] Galanski, M.; Arion, V. B.; Jakupec, M. A.; Keppler, B. K.; *Current pharmaceutical design,* **2003**, *9*, 2078-2089.

[33] Reisner, E.; Arion, V. B.; Keppler, B. K.; Pombeiro, A. J. L.; *Inorganica Chimica Acta,* **2008**, *361*, 1569-1583.

[34] Duan, L.; Fischer, A.; Xu, Y.; Sun, L.; *Journal of the American Chemical Society,* **2009**, *131*, 10397-10399.

[35] Dragutan, I.; Dragutan, V.; Demonceau, A.; *Molecules,* **2015**, *20*, 17244.

[36] Bergamo, A.; Zorzet, S.; Gava, B.; Sorc, A.; Alessio, E.; Iengo, E.; Sava, G.; *Anti-Cancer Drugs,* **2000**, *11*, 665-672.

[37a] Leijen, S.; Burgers, S. A.; Baas, P.; Pluim, D.; Tibben, M.; van Werkhoven, E.; Alessio, E.; Sava, G.; Beijnen, J. H.; Schellens, J. H. M.; *Investigational New Drugs,* **2015**, *33*, 201-214;

[37b] Rademaker-Lakhai, J. M.; van den Bongard, D.; Pluim, D.; Beijnen, J. H.; Schellens, J. H.; *Clinical cancer research : an official journal of the American Association for Cancer Research,* **2004**, *10*, 3717-3727.

[38] Lentz, F.; Drescher, A.; Lindauer, A.; Henke, M.; Hilger, R. A.; Hartinger, C. G.; Scheulen, M. E.; Dittrich, C.; Keppler, B. K.; Jaehde, U.; *Anticancer Drugs,* **2009**, *20*, 97-103.

[39] Burris, H. A.; Bakewell, S.; Bendell, J. C.; Infante, J.; Jones, S. F.; Spigel, D. R.; Weiss, G. J.; Ramanathan, R. K.; Ogden, A.; Von Hoff, D.; *ESMO Open,* **2016**, *1*, e000154.

[40] Trondl, R.; Heffeter, P.; Kowol, C. R.; Jakupec, M. A.; Berger, W.; Keppler, B. K.; *Chemical Science,* **2014**, *5*, 2925-2932.

[41] Maeda, H.; Wu, J.; Sawa, T.; Matsumura, Y.; Hori, K.; *Journal of controlled release : official journal of the Controlled Release Society,* **2000**, *65*, 271-284.

[42a] Piccioli, F.; Sabatini, S.; Messori, L.; Orioli, P.; Hartinger, C. G.; Keppler, B. K.; *Journal of Inorganic Biochemistry,* **2004**, *98*, 1135-1142;

[42b] Timerbaev, A. R.; Foteeva, L. S.; Rudnev, A. V.; Abramski, J. K.; Połeć-Pawlak, K.; Hartinger, C. G.; Jarosz, M.; Keppler, B. K.; *ELECTROPHORESIS,* **2007**, *28*, 2235-2240.

[43a] Heffeter, P.; Bock, K.; Atil, B.; Reza Hoda, M. A.; Korner, W.; Bartel, C.; Jungwirth, U.; Keppler, B. K.; Micksche, M.; Berger, W.; Koellensperger, G.; *Journal of biological inorganic chemistry : JBIC : a publication of the Society of Biological Inorganic Chemistry,* **2010**, *15*, 737-748;

[43b] Clarke, M. J.; *Coordination Chemistry Reviews,* **2003**, *236*, 209-233.

[44] Flocke, L. S.; Trondl, R.; Jakupec, M. A.; **2016**, *34*, 261-268.

[45a] Clarke, M. J.; Zhu, F.; Frasca, D. R.; *Chemical reviews,* **1999**, *99*, 2511-2534;

[45b] Smith, C. A.; Sutherland-Smith, A. J.; Kratz, F.; Baker, E. N.; Keppler, B. H.; *JBIC Journal of Biological Inorganic Chemistry,* **1996**, *1*, 424-431.

[46] Heffeter, P.; Atil, B.; Kryeziu, K.; Groza, D.; Koellensperger, G.; Körner, W.; Jungwirth, U.; Mohr, T.; Keppler, B. K.; Berger, W.; *European Journal of Cancer,* **2013**, *49*, 3366-3375.

[47] Scolaro, C.; Bergamo, A.; Brescacin, L.; Delfino, R.; Cocchietto, M.; Laurenczy, G.; Geldbach, T. J.; Sava, G.; Dyson, P. J.; *Journal of medicinal chemistry,* **2005**, *48*, 4161-4171.

[48] Suss-Fink, G.; *Dalton transactions (Cambridge, England : 2003),* **2010**, *39*, 1673-1688.

[49] Dougan, S. J.; Sadler, P. J.; *CHIMIA International Journal for Chemistry,* **2007**, *61*, 704-715.

[50] Casini, A.; Hartinger, C. G.; Nazarov, A. A.; Dyson, P. J., in *Medicinal Organometallic Chemistry* (Eds.: G. Jaouen, N. Metzler-Nolte), Springer Berlin Heidelberg, Berlin, Heidelberg, **2010**, pp. 57-80.

[51a] Romero-Canelón, I.; Sadler, P. J.; *Inorganic Chemistry,* **2013**, *52*, 12276-12291;
[51b] Loughrey, B. T.; Williams, M. L.; Healy, P. C.; Innocenti, A.; Vullo, D.; Supuran, C. T.; Parsons, P. G.; Poulsen, S. A.; *Journal of biological inorganic chemistry : JBIC : a publication of the Society of Biological Inorganic Chemistry,* **2009**, *14*, 935-945;
[51c] Gao, F.; Chao, H.; Wang, J. Q.; Yuan, Y. X.; Sun, B.; Wei, Y. F.; Peng, B.; Ji, L. N.; *Journal of biological inorganic chemistry : JBIC : a publication of the Society of Biological Inorganic Chemistry,* **2007**, *12*, 1015-1027.

[52] Jungwirth, U.; Kowol, C. R.; Keppler, B. K.; Hartinger, C. G.; Berger, W.; Heffeter, P.; *Antioxidants & redox signaling,* **2011**, *15*, 1085-1127.

[53] Medici, S.; Peana, M.; Nurchi, V. M.; Lachowicz, J. I.; Crisponi, G.; Zoroddu, M. A.; *Coordination Chemistry Reviews,* **2015**, *284*, 329-350.

[54a] Peacock, A. F. A.; Sadler, P. J.; *Chemistry – An Asian Journal,* **2008**, *3*, 1890-1899;
[54b] van Rijt, S. H.; Peacock, A. F. A.; Johnstone, R. D. L.; Parsons, S.; Sadler, P. J.; *Inorganic Chemistry,* **2009**, *48*, 1753-1762.

[55] A. Taylor, N. C.; *Cancer Studies 2* **1953**, *36*, 3565.

[56] Katsaros, N.; Anagnostopoulou, A.; *Critical reviews in oncology/hematology,* **2002**, *42*, 297-308.

[57a] Dadci, L.; Elias, H.; Frey, U.; Hoernig, A.; Koelle, U.; Merbach, A. E.; Paulus, H.; Schneider, J. S.; *Inorganic Chemistry,* **1995**, *34*, 306-315;
[57b] Geldmacher, Y.; Oleszak, M.; Sheldrick, W. S.; *Inorganica Chimica Acta,* **2012**, *393*, 84-102.

[58] Wellington, K. W.; *RSC Advances,* **2015**, *5*, 20309-20338.

[59a] Brenner, A. K.; Reikvam, H.; Lavecchia, A.; Bruserud, O.; *Molecules,* **2014**, *19*, 18414-18447;

[59b] Brezak, M. C.; G Kasprzyk, P.; Galcera, M. O.; Lavergne, O.; Prevost, G., *CDC25 Inhibitors as Anticancer Agents Are Moving Forward, Vol. 8*, **2009**;

[59c] Contour-Galcera, M. O.; Sidhu, A.; Prevost, G.; Bigg, D.; Ducommun, B.; *Pharmacology & therapeutics,* **2007**, *115*, 1-12.

[60] Fila, C.; Metz, C.; van der Sluijs, P.; *The Journal of biological chemistry,* **2008**, *283*, 21714-21724.

[61] Ji, Y. B.; Qu, Z. Y.; Zou, X.; *Experimental and toxicologic pathology : official journal of the Gesellschaft fur Toxikologische Pathologie,* **2011**, *63*, 69-78.

[62] Didry, N.; Dubreuil, L.; Pinkas, M.; *Die Pharmazie,* **1994**, *49*, 681-683.

[63] Likhitwitayawuid, K.; Kaewamatawong, R.; Ruangrungsi, N.; Krungkrai, J.; *Planta Med,* **1998**, *64*, 237-241.

[64] Checker, R.; Sharma, D.; Sandur, S. K.; Subrahmanyam, G.; Krishnan, S.; Poduval, T. B.; Sainis, K. B.; *Journal of Cellular Biochemistry,* **2010**, *110*, 1082-1093.

[65] McKallip, R. J.; Lombard, C.; Sun, J.; Ramakrishnan, R.; *Toxicology and Applied Pharmacology,* **2010**, *247*, 41-52.

[66] Son, T. G.; Camandola, S.; Arumugam, T. V.; Cutler, R. G.; Telljohann, R. S.; Mughal, M. R.; Moore, T. A.; Luo, W.; Yu, Q.-S.; Johnson, D. A.; Johnson, J. A.; Greig, N. H.; Mattson, M. P.; *Journal of Neurochemistry,* **2010**, *112*, 1316-1326.

[67] Liu, Y.; Cai, Y.; He, C.; Chen, M.; Li, H.; *The American journal of Chinese medicine,* **2017**, *45*, 423-441.

[68] Kawiak, A.; Piosik, J.; Stasilojc, G.; Gwizdek-Wisniewska, A.; Marczak, L.; Stobiecki, M.; Bigda, J.; Lojkowska, E.; *Toxicol Appl Pharmacol,* **2007**, *223*, 267-276.

[69] Acharya, B. R.; Bhattacharyya, B.; Chakrabarti, G.; *Biochemistry,* **2008**, *47*, 7838-7845.

[70] S.N. Fedorov, L. K. S., A.S. Kuzmich, S.G. Polonik; *Open Glycoscience,* **2011**, *4*, 1-5.

[71] Turrens, J. F.; *The Journal of Physiology,* **2003**, *552*, 335-344.

[72] Castro, F. A.; Mariani, D.; Panek, A. D.; Eleutherio, E. C.; Pereira, M. D.; *PloS one,* **2008**, *3*, e3999.

[73] Fujii, N.; Yamashita, Y.; Arima, Y.; Nagashima, M.; Nakano, H.; *Antimicrobial agents and chemotherapy,* **1992**, *36*, 2589-2594.

[74] Lopez, L.; Javier Vaquera Garcia, J.; Galindo, A.; Silva, Y., *Ultrasonic and Microwave Assisted Synthesis of Nitrogen-Containing Derivatives of Juglone as Potential Antibacterial Agents, Vol. 11*, **2014**.

[75] Vijayalakshmi, J.; Rajan, S. S.; Srinivasan, R.; *Acta Crystallographica Section C,* **1987**, *43*, 2375-2377.

[76] Cradwick, P. D.; Hall, D.; *Acta Crystallographica Section B,* **1971**, *27*, 1468-1470.

[77] Janiak, C.; *Journal of the Chemical Society, Dalton Transactions,* **2000**, 3885-3896.

[78] Hernandez-Munoz, L. S.; Gomez, M.; Gonzalez, F. J.; Gonzalez, I.; Frontana, C.; *Organic & Biomolecular Chemistry,* **2009**, *7*, 1896-1903.

[79] Werner, H.; Zenkert, K.; *Journal of Organometallic Chemistry,* **1988**, *345*, 151-166.